University of Alberta

A Biochemical and Molecular Genetic Approach to Confirming the Clinical Diagnosis of Choroideremia

by

Dean Yon Mah

A thesis submitted to the Faculty of Graduate Studies and Research in partial fulfillment of the requirements for the degree of Master of Science in

Medical Sciences - Ophthalmology

Edmonton, Alberta

Fall, 1999

National Library of Canada
Acquisitions and Bibliographic Services
395 Wellington Street
Ottawa ON K1A 0N4
Canada

Bibliothèque nationale du Canada
Acquisitions et services bibliographiques
395, rue Wellington
Ottawa ON K1A 0N4
Canada

Your file Votre référence

Our file Notre référence

The author has granted a non-exclusive licence allowing the National Library of Canada to reproduce, loan, distribute or sell copies of this thesis in microform, paper or electronic formats.

L'auteur a accordé une licence non exclusive permettant à la Bibliothèque nationale du Canada de reproduire, prêter, distribuer ou vendre des copies de cette thèse sous la forme de microfiche/film, de reproduction sur papier ou sur format électronique.

The author retains ownership of the copyright in this thesis. Neither the thesis nor substantial extracts from it may be printed or otherwise reproduced without the author's permission.

L'auteur conserve la propriété du droit d'auteur qui protège cette thèse. Ni la thèse ni des extraits substantiels de celle-ci ne doivent être imprimés ou autrement reproduits sans son autorisation.

0-612-47062-8

Canada

University of Alberta

Library Release Form

Name of Author: Dean Yon Mah

Title of Thesis: A Biochemical and Molecular Genetic Approach to Confirming the Clinical Diagnosis of Choroideremia

Degree: Master of Science

Year this Degree Granted: 1999

Permission is hereby granted to the University of Alberta Library to reproduce single copies of this thesis and to lend or sell such copies for private, scholarly, or scientific research purposes only.

The author reserves all other publication and other rights in association with the copyright in the thesis, and except as hereinbefore provided, neither the thesis nor any substantial portion thereof may be printed or otherwise reproduced in any material form whatever without the author's prior written permission.

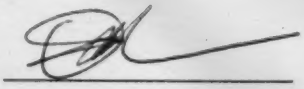

Kingsview Apartments
Apartment #808
1725 Riverside Drive
Ottawa, Ontario
K1G 0E6

August 27, 1999.

University of Alberta

Faculty of Graduate Studies and Research

The undersigned certify that they have read, and recommend to the Faculty of Graduate Studies and Research for acceptance, a thesis entitled **A Biochemical and Molecular Genetic Approach to Confirming the Clinical Diagnosis of Choroideremia** submitted by Dean Yon Mah in partial fulfillment of the requirements for the degree of Master of Science in Medical Sciences - Ophthalmology.

Dr. Ian M. MacDonald

Dr. Michael Walter

Dr. Luc Berthiaume

Abstract

Choroideremia (CHM) is an X-linked form of retinal degeneration leading to progressive blindness in affected males. Female carriers are usually asymptomatic, but can be identified by subtle retinal pigmented epithelium abnormalities. The gene responsible for CHM has been cloned, and encodes Rab escort protein-1 (REP-1) necessary for proper trafficking of cellular vesicles.

As all cases of CHM to date result in the premature truncation of the REP-1 protein, the work presented here suggests that immunoblot analysis is a practical and reliable method for testing suspected CHM males. Protein extracted from lymphocytes or lymphoblastoid cells was subjected to REP-1 detection using a highly specific REP-1 monoclonal antibody. In those cases where REP-1 protein was absent, the specific REP-1 gene mutation was identified and characterized. Molecular genetic data validates the results of the immunoblot analysis and allows for carrier and prenatal testing in CHM families.

Acknowledgements

There are many people that I must acknowledge for their tremendous support given to me throughout my project. I would first like to express my deepest appreciation to Dr. Ian MacDonald, whose encouragement and guidance helped make my graduate career a rewarding and fulfilling experience. I will always be indebted to him, for allowing me the opportunity to achieve what I have thus far, and for teaching me valuable lessons which will help me in the future. I also owe a great deal to Dr. Michael Walter for his continuous support and advice, which were much needed throughout my studies. I would like to thank Dr. Luc Berthiaume for his knowledge and expertise which were invaluable in my research. Thanks to the Ocular Genetics laboratory, for always being there for me, and making each and every day in the lab memorable and enjoyable. I would also like to gratefully acknowledge Dr. Heather McDermid, for initially giving me my start in molecular genetics, and for giving me the self-confidence to continue on. Lastly, I owe so much to my family, especially my Mom and Dad, for their numerous sacrifices which have enabled me to pursue my goals and dreams. I never could have achieved anything without their unconditional love and understanding throughout my life.

Table of contents

Introduction **1**

Clinical 1
Fundus examination 2
Histopathology 3
Fluorescein angiogram 5
Pathogenesis 5
Positional cloning of the human X-linked CHM gene 6
Rab proteins 7
Rabs and SNAREs 7
The Rab cycle 8
Prenylation 9
FT and GGT I 10
Rab GGT or GGT II 11
Rab escort protein (REP) 12
REP-1 associates with Rab proteins 12
Geranylgeranyl addition 13
REP-1 acts as a molecular chaperone 14
REP-1 and Rab GDI are similar in structure and function 15
REP-1 vs. REP-2 16

Materials and Methods **18**

Families
Family 1 19
Family 2 20
Family 3 21
Family 4 22
Family 5 23
B95-8 cell line maintenance and Epstein-Barr Virus (EBV) production 24
Creation of lymphoblastoid cell lines 24
Protein extraction 25
Western analysis 26
DNA extraction from peripheral blood 27
Single-stranded conformation polymorphism (SSCP) 28
Direct DNA sequencing 29
RNA isolation and reverse transcriptase (RT) PCR 29
Sequence analysis of RT-PCR products 30

Results **31**

Western analysis 31
Family1 31
Family 2 31

Family 3 32
Family 4 32
Family 5 32
SSCP analysis 32
Family 1 33
Family 2 33
Family 3 33
Family 4 33
DNA sequence analysis 33
Family1 34
Family 2 34
Family 3 34
Family 4 34
RT-PCR 35
Direct sequencing of the RT-PCR product 35

Discussion **37**

Described mutations 37
Future work
Continued mutation detection 39
X-inactivation of the REP-1 gene 40
A REP protein family? 41
Mutations in GDI : A GDI protein family 41
Animal models 42
Gene therapy 43
Conclusion 44

Reference List **46**

List of Tables

Table 1-1	Location and function of Rab proteins in mammalian cells	54
Table 2-1	Oligonucleotide primers used for PCR amplification of CHM exons	55
Table 4-1	REP-1 gene mutations discovered in this study	56

List of Figures

Figure 1-1	Cross-sectional diagram of the retina	57
Figure 1-2	Fundus photograph taken from an affected male	58
Figure 1-3	Fundus photograph taken from a carrier female	59
Figure 1-4	Position of the CHM gene on the X-chromosome and structure of the open reading frame	60
Figure 1-5	Rab protein involvement in membrane trafficking	61
Figure 1-6	The role of the REP-1 protein in the geranylgeranylation of Rab proteins	62
Figure 3-1	Western analysis of serial dilutions of lymphocyte protein	63
Figure 3-2	Western analysis performed on lymphocyte protein from Family 1 individuals	64
Figure 3-3	Western analysis performed on lymphoblast protein from Family 2 individuals	65
Figure 3-4	Western analysis performed on lymphoblast protein from Family 3 individuals	66
Figure 3-5	Western analysis performed on lymphocyte protein from Family 4 individuals	67
Figure 3-6	Western analysis performed on lymphocyte protein from Family 5 individuals	68
Figure 3-7	SSCP analysis of exon 7 from Family 1 individuals	69
Figure 3-8	SSCP analysis of exon 5 from Family 2 individuals	70
Figure 3-9	SSCP analysis of exon 6 from Family 3 individuals	71

Figure 3-10	SSCP analysis of exon 1 from Family 4 individuals	72
Figure 3-11	Sequence analysis of exon 7 from Family 1 individuals	73
Figure 3-12	Sequence analysis of exon 5 from Family 2 individuals	74
Figure 3-13	Sequence analysis of exon 6 from Family 3 individuals	75
Figure 3-14	Sequence analysis of exon 1 from Family 4 individuals	76
Figure 3-15	PCR amplification of exons 4, 5, 8 and 9 from individuals from Family 5	77
Figure 3-16a	Location of PCR primers used for RT-PCR on individual III:1 from Family 5	78
Figure 3-16b	RT-PCR results from individual III:1 from Family 5	78
Figure 3-17	Direct sequencing of the RT-PCR product from individual III:1 from Family 5	79
Figure 4-1	Locations of previously published mutations and those described in this work	80

List of Abbreviations

β-Me	β-mercaptoethanol
BSA	bovine serum albumin
C-terminus	carboxyl terminus
CHM	choroideremia
DMEM	Dulbecco's Modified Eagle Medium
DNA	deoxyribonucleic acid
dATP	deoxyadenosine 5' triphosphate
dGTP	deoxyguanosine 5' triphosphate
dCTP	deoxycytidine 5' triphosphate
dTTP	deoxythymidine 5' triphosphate
EBV	Epstein-Barr virus
EDTA	ethylenediaminetetra-acetic acid
ER	endoplasmic reticulum
ERG	electroretinogram
FT	farnesyltransferase
GAP	GTPase activating protein
GDF	GDI-displacement factor
GDI	GDP-dissociation inhibitor
GDP	guanosine 5' diphosphate
GEF	guanine nucleotide exchange factor
GG	geranylgeranyl
GGPP	geranylgeranylpyrophosphate
GGT	geranylgeranyltransferase
GTB	glycerol tolerant buffer
GTP	guanosine 5' triphosphate
GTPase	guanosine 5' triphosphatase
HEPES	4-(2-hydroxyethyl)-1-piperazineethane sulfonic acid
kDa	kilodaltons
kb	kilobases
MOPS	3-(N-morpholino) propane-sulfonic acid
N-terminus	amino terminus
OD	oculus dexter (right eye)
OS	oculus sinister (left eye)
OU	oculus uterque (both eyes)
PBS	phosphate-buffered saline
PCR	polymerase chain reaction
RBC	red blood cell
REP	Rab Escort Protein
RNA	ribonucleic acid
RPE	retinal pigment epithelium
RT-PCR	reverse transcriptase PCR
SDS	sodium dodecyl sulphate
SEM	scanning electron microscopy

SNARE	α-soluble *N*-ethylmaleimide sensitive factor attachment protein receptors
SSCP	single-stranded conformation polymorphism
Taq	*Thermus aquaticus*
TBE	TRIS-borate/EDTA
TE	TRIS/EDTA
TEM	transmission electron microscopy
TGN	trans-Gogli network
TRIS	Tris(hydroxymethyl)aminomethane
WBC	white blood cell

Introduction

Clinical

Choroideremia (CHM) is an X-linked hereditable blinding disorder. Mauthner (Mauthner, 1871) provided the first clinical description of choroideremia and noted absence of a distinct choroid layer in those afflicted (Fig. 1-1). The disease begins usually in the adolescent years and progresses with age (McCulloch and McCulloch, 1948). Affected males present first with nightblindness (McCulloch and McCulloch, 1948; Carr and Noble, 1980; Sorsby et al., 1952). Ring scotomas form in the mid-periphery of the visual field followed by loss of peripheral vision (McCulloch and McCulloch, 1948; Carr and Noble, 1980; Sorsby et al., 1952; Pameyer et al., 1960). Central visual acuity is maintained until quite late in the disease, with macular sparing (McCulloch and McCulloch, 1948; Carr and Noble, 1980; Francois, 1968; Kurstjens, 1965; Noble et al., 1977; Rodrigues et al., 1984). Affected males show an abnormal electroretinogram (ERG), with reduced or absent scotopic component and elevated dark-adaptation thresholds (Francois, 1968; Noble et al., 1977; Kurstjens, 1965; Pameyer et al., 1960). Gradually, central visual acuity decreases and the patient is left completely blind by their senior years (McCulloch and McCulloch, 1948; Francois, 1968; Sorsby et al., 1952).

Female carriers are asymptomatic in most cases. No abnormalities are seen with respect to the visual fields, ERG findings or visual acuity (Carr and Noble, 1980; Francois, 1968; Noble et al., 1977; Rodrigues et al., 1984). There are rare cases in which female carriers exhibit progressive signs of CHM and vision loss (Harris and Miller, 1968; Fraser and Friedmann, 1968; Flannery et al., 1990; Forsius et al., 1977).

It is possible that these rare occurrences can be explained by the Lyon hypothesis, when the normal allele in the female carrier could by chance be inactivated in developing eye tissues (Fraser and Friedmann, 1968; Harris and Miller, 1968).

Fundus examination

Males affected with CHM initially present with early fundus changes which are commonly described as pigment mottling of the "salt and pepper" type (Carr and Noble, 1980; Noble et al., 1977). Areas of hypo- and hyperpigmentation are seen in the midperiphery of the retina (McCulloch and McCulloch, 1948; Carr and Noble, 1980; Francois, 1968; Noble et al., 1977; Kurstjens, 1965; Pameyer et al., 1960; Sorsby et al., 1952). Areas of hyperpigmentation are seen as clumps of irregular dark patches of pigment granules (McCulloch and McCulloch, 1948). Areas of hypopigmentation appear as pale patches of thinned retinal pigment epithelium (RPE), through which underlying sclera can be seen, continuing until all pigmentation is lost and the entire midperiphery is seen as a ring of white sclera (McCulloch and McCulloch, 1948). This marked depigmentation progresses to the far peripheral regions of the retina, at which time peripheral vision decreases and is eventually lost (McCulloch and McCulloch, 1948). During this period of retinal degeneration, larger choroidal vessels running over the sclera are exposed; these eventually disappear, beginning in the periphery toward the macula (Sorsby et al., 1952). At its end stages, complete atrophy of the choroid and retina occurs, and the fundus appears bare white and glistening as the underlying sclera is entirely visible (Fig. 1-2) (McCulloch and McCulloch, 1948; Carr and Noble, 1980; Sorsby et al., 1952; Francois, 1968; Kurstjens, 1965; Noble et al., 1977). Throughout the degenerative process, retinal

vessels, optic disk and nerve appear normal until the late stages of the disease (Francois, 1968; Rodrigues et al., 1984; Kurstjens, 1965). It is important to note that although the chorioretinal atrophy is progressive, the severity and its progression can vary between individuals and families (Francois, 1968; Noble et al., 1977; Sorsby et al., 1952).

Female carriers do exhibit fundus findings such as subtle RPE abnormalities in the midperiphery, similar to those seen in the affected male (Fig. 1-3) (Carr and Noble, 1980; Francois, 1968; Noble et al., 1977; Rodrigues et al., 1984). These signs are progressive, but not to the extent of those seen in the affected male. The fundus abnormalities are similar to those seen early in the affected male, with patchy areas of irregular pigmentation in the midperiphery of the retina.

Histopathology

Histopathological findings have contributed to our understanding of the pathogenesis of CHM. Examination of an eye from an affected 19 year old male by Rodrigues showed marked degeneration of midperipheral and peripheral areas of the retina, with loss of RPE, Bruch's membrane and choriocapillaris (Rodrigues et al., 1984). Bone spicule formation in the midperipheral and peripheral areas indicated massive degeneration (Rodrigues et al., 1984). In addition, cells resembling macrophages were seen in the RPE and outer retina, with outer segment discs attached to the plasma membrane of the macrophage-like cells. The authors suggested that CHM could result from a defect in phagocytosis of discs (Rodrigues et al., 1984). Other histopathological results by both Rafuse (Rafuse and McCulloch, 1968) and Ghosh (Ghosh and McCulloch, 1980) on donor eyes taken from males with advanced CHM

showed retinal disorganization in the periphery and midperiphery (Rafuse and McCulloch, 1968). In these areas, the choroid was severely atrophic, with complete loss of choriocapillaris, rod and cone receptors (Rafuse and McCulloch, 1968; Ghosh and McCulloch, 1980). Within the macular region the choroid was present, however RPE and Bruch's membrane were both absent (Rafuse and McCulloch, 1968). Interestingly, studies have also found changes in the nerve fiber layer. In one affected male 67 years of age, the nerve fiber layer was degenerate (Rafuse and McCulloch, 1968). Moreover, Ghosh (Ghosh and McCulloch, 1980) noticed gliosis in the ganglion cell and nerve fiber layer, in addition to a "pre-retinal membrane" internal to that of the internal limiting membrane, composed of fibrils and cells, which could presumably play a role in early visual field loss (Ghosh and McCulloch, 1980). These histopathological findings reaffirm that advanced stages of CHM show definite loss of choroid, RPE and Bruch's, with secondary loss of the photoreceptors and disorganization of the entire retina.

In female carriers, similar degenerative retinal findings were not seen. However, upon closer examination by electron microscopy, specific histopathological abnormalities were noticed (MacDonald et al., 1997). Transmission electron microscopy (TEM) showed some loss of villi in RPE cells (MacDonald et al., 1997). Scanning EM (SEM) revealed the same loss of villi, in addition to abnormal RPE cell structure and organization throughout the fundus. Normal photoreceptors were seen and the remainder of the retina seemed normal (MacDonald et al., 1997).

Fluorescein angiogram

Fluorescein angiography has been used to specifically identify which regions of the retina undergo atrophy first, the results of which could determine the pathogenesis of the disease. Fluorescein angiography examination in affected males showed early atrophy of the choriocapillaris, with only the large underlying choroidal vessels remaining (Carr and Noble, 1980). Loss of choriocapillaris first appeared in the midperiphery of the fundus and extended outward into the periphery, sparing the macula until late in the onset of the disease (Carr and Noble, 1980; Noble et al., 1977). A fluorescein angiogram of the female carrier showed only pigmentary irregularities, with no choriocapillaris atrophy (Noble et al., 1977). The choriocapillaris seemed to be present throughout the female fundus, perhaps explaining the difference in disease prognosis (Noble et al., 1977).

Pathogenesis

There has been much discussion on the pathogenesis of CHM and which regions of the retina are specifically affected. CHM pathogenesis seems to be related to initial choroid degeneration (Carr and Noble, 1980). The characteristic progression from the early stages of the disease to the advanced state in the affected males along with the RPE irregularities seen in the female carrier (abnormal RPE cell shape and RPE pigment "mottling") suggest that CHM may be a disorder of the RPE, with secondary atrophy of the choriocapillaris and retina (MacDonald et al., 1997). Based on histopathological findings showing loss of rods and cones, it may be that this loss is secondary to choriocapillaris loss and transport defect. It may soon become evident when the underlying biochemical defect of CHM is described that transport between

RPE and the retina and/or choroid may be disrupted. This may explain the resulting retinal degeneration seen in CHM (MacDonald et al., 1997).

Positional cloning of the human X-linked CHM gene

The position of the CHM gene was first localized to the X-chromosome based on the sex-linked pattern of inheritance identified in families afflicted with the disorder (McCulloch and McCulloch, 1948). Linkage studies initially placed the CHM gene at the broad region of Xq13-21 (Lewis et al., 1985; Nussbaum et al., 1985). Other linkage data by numerous additional groups later confirmed these results (Gal et al., 1986; Jay et al., 1986; Lesko et al., 1987; Rosenberg et al., 1986; MacDonald et al., 1987; Sankila et al., 1987; Wright et al., 1990). Characterization of chromosomal deletions associated with syndromes involving CHM (Rosenberg et al., 1986; Nussbaum et al., 1987; Hodgson et al., 1987; Schwartz et al., 1988; Merry et al., 1989; Cremers et al., 1989) and molecular studies involving a CHM female with a balanced de novo X;13 translocation (Cremers et al., 1989; Merry et al., 1990; Siu et al., 1990) helped further refine the map location of the gene. Eventually, a 45 kb segment of genomic DNA overlapping the majority of deletions associated with CHM was cloned and characterized (Cremers et al., 1990). Further study and isolation of single copy sequences from this segment in addition to similar work from other groups led to the isolation of partial candidate CHM DNA clones (Cremers et al., 1990b; Merry et al., 1992).

Subsequent work has led to the complete cloning and characterization of the coding region of the CHM gene (Fig. 1-4) (van Bokhoven et al., 1994b). The gene is composed of 15 exons which span approximately 150 kb of genomic DNA at Xq21.2.

Study of the exact intron-exon boundaries has established that exon sizes range from 63 nucleotides to 3.4 kb. The cDNA sequence is 5.6 kb in length and contains an open reading frame encoding a protein which is 653 amino acids in length. Insight into the functional significance of the human CHM gene came when protein homology was discovered between this CHM gene product and an enzyme subunit involved in the attachment of lipid moieties to Rab proteins (Seabra et al., 1992a).

Rab proteins

Rab proteins are members of the Ras superfamily of GTPases and function to regulate membrane fusion events which occur during vesicular transport (Nuoffer and Balch, 1994; Pfeffer, 1994; Novick and Zerial, 1997b). In mammalian cells, there have been over 30 members of the Rab family which have been identified to date (Table 1-1). Each Rab protein has been localized to a different subcellular compartment of exocytic and endocytic pathways, as each member of the Rab protein family plays a specific role in regulating different vesicular transport events in a number of various cell types (Novick and Zerial, 1997b). For example, two Rab members, termed 1A and 1B are involved in vesicular trafficking from the endoplasmic reticulum to the Golgi apparatus, whereas a Rab8 is localized at late Golgi compartments and functions in regulating transport to the plasma membrane (Nuoffer and Balch, 1994; Novick and Zerial, 1997b).

Rabs and SNAREs

Rab proteins regulate vesicular traffic not by directly targeting vesicles to their target membranes and promoting fusion, but by mediating interaction between what are known as α-soluble *N*-ethylmaleimide sensitive factor attachment protein receptors

(SNAREs) (Novick and Zerial, 1997b; Sogaard et al., 1994; Pfeffer, 1994). SNAREs are anchored integral membrane protein receptors which are located on vesicles (v-SNAREs) and their target membranes (t-SNAREs). SNAREs specifically interact with each other to ensure that the appropriate vesicle docks and promotes fusion with target membranes (Overmeyer et al., 1998). Rab proteins are necessary for the correct assembly of the v- and t-SNARE complex, working to facilitate proper SNARE pairing and subsequent vesicular targeting at the correct time and location (Sogaard et al., 1994; Pfeffer, 1994; Novick and Brennwald, 1993).

The Rab cycle

Rabs are found in the cytosol bound to GDP, and are kept in an inactive conformation by Rab GDP-dissociation inhibitor (Rab GDI). Rab GDI forms a stable complex with Rab-GDP to inhibit GDP→GTP exchange and protect the hydrophobic geranylgeranyl lipid groups in order that Rabs remain soluble in the aqueous cytosolic environment (Matsui et al., 1990; Ullrich et al., 1994b; Soldati et al., 1994). By doing so, Rab-GDP remains soluble within the cytoplasm and in the inactive state, preventing improper and indiscriminate membrane binding. Before Rab proteins can function, they must first be dissociated from Rab GDI. Recently, a novel membrane protein has been described which can detach GDI from endosomal Rab proteins (Dirac-Svejstrup et al., 1997), and may be one of a number of proteins responsible for this specific activity. Once Rab-GDP is free from GDI, it is able to bind its proper cellular compartment and integrates itself within the membrane (Ullrich et al., 1994b; Soldati et al., 1994). Following this, GDP is replaced by GTP, catalyzed by a specific guanine nucleotide exchange factor (GEF), rendering Rab in an active state. The Rab protein is now

stably bound to the organelle membrane and resistant to removal by Rab GDI (Ullrich et al., 1994b; Soldati et al., 1994). The process of vesicular transport, with SNARE involvement, is now initiated. Vesicular budding occurs, vesicles are transported to their target membranes resulting in membrane fusion, which releases vesicular contents into the acceptor compartment. Once this process is complete, a GTPase activating protein or GAP (Fukui et al., 1997) activates the GTPase function of the Rab protein, resulting in the cleavage of a phosphate group from the GTP molecule bound to Rab. This enables Rab-GDI to bind Rab-GDP, delivering GDP-bound Rab back to its original membrane location so that the entire process can occur once more (Fig. 1-5).

Prenylation

Even before the Rab cycle previously described can occur, newly synthesized Rab proteins must first ensure that they are localized to the appropriate organelle membrane and maintain stable hydrophobic interaction within the cytoplasmic leaflet. In order to do so, nascent Rabs must first be modified by a process known as prenylation. This process refers to the covalent attachment of isoprenyl groups onto cysteine residues located near the C-terminus (Casey and Seabra, 1996; Clarke, 1992; Zhang and Casey, 1996; Glomset and Farnsworth, 1994). These isoprenyl groups which are transferred to the proteins are attached via a thioether chemical bond, and include either a 15-carbon farnesyl group or a 20-carbon geranylgeranyl (GG) group. Due primarily to the hydrophobicity of these lipid chains, prenylation promotes interactions with other cellular proteins, and is essential for protein-membrane association. Prenylation is not uncommon, with greater than 0.5% of all cellular

protein being modified in this manner (Epstein et al., 1991). Prenylated proteins have been implicated in a number of significant cellular roles such as signal transduction and, as already mentioned, intracellular vesicular trafficking.

FT and GGT I

There are essentially two classes of prenyltransferases (Casey and Seabra, 1996; Clarke, 1992; Zhang and Casey, 1996; Glomset and Farnsworth, 1994). The first group is referred to as the CAAX prenyltransferase and contains two members, farnesyltransferase (FT) and geranylgeranyltransferase I (GGT I). This group is so named because of their ability to recognize a CAAX motif representing four amino acids near the C-terminus of the protein to be modified. The C represents the cysteine residue to which the isoprenyl group is actually attached and the A positions generally represent aliphatic amino acids. The X residue specifies which prenyltransferase actually modifies the protein: if X is a serine, methionine, alanine or glutamine residue, the protein receives a farnesyl group; if the X is a leucine residue, then GGT I acts to modify the protein with the attachment of a GG group (Casey and Seabra, 1996; Moores et al., 1991; Matsui et al., 1990).

FT and GGT I have both been characterized and purified from rat brain (Beranger et al., 1994) and bovine brain (Moores et al., 1991) tissues, respectively. FT is a heterodimer composed of a 48 kDa α-subunit and a 45 kDa β-subunit. Short peptide recognition experiments have shown that the CAAX motif alone is sufficient for FT recognition and farnesyl attachment (Beranger et al., 1994; Moores et al., 1991). Proteins which are known to be farnesylated include Ras proteins, and transducin and rhodopsin kinase, two components involved in the phototransduction cascade (Zhang

and Casey, 1996). GGT I is also composed of two subunits, a 48 kDa α-subunit which is identical to that of the α-subunit from FT, in addition to a 43 kDa β-subunit. Examples of proteins modified by GGT I include Ras-related small GTPases including Rac and Rho (Zhang and Casey, 1996). GGT I binding requirements are similar to those of FT, in that the heterodimer is also capable of recognizing and prenylating short peptides containing only the CAAX motif (Matsui et al., 1990; Moores et al., 1991).

Rab GGT or GGT II

As previously mentioned, Rab proteins must be prenylated in order to properly interact with intracellular membranes. Without this modification, unprenylated Rabs will remain cytosolic and inactive within the cell (Khosravi-Far et al., 1991; Kinsella and Maltese, 1992). However, unlike other proteins which are modified by the CAAX prenyltransferases, Rab proteins do not contain this motif. Instead, the majority of Rabs contain a CC or CXC motif found at the C-terminus (Khosravi-Far et al., 1991) (Farnsworth et al., 1991; Moores et al., 1991), and require a prenyltransferase distinct from that of the CAAX prenyltransferases (Moores et al., 1991; Khosravi-Far et al., 1991; Horiuchi et al., 1991; Kinsella and Maltese, 1992; Farnsworth et al., 1991). This second class of enzymes is referred to as geranylgeranyltransferase II (GGT II) or Rab GGT. Although the end result of the GGT II enzymatic reaction is still the prenylation at cysteine residues, the reaction itself is much more complex.

Rab GGT activity was first purified from rat brain tissues as an enzyme able to catalyze the transfer of GG from a GG pyrophosphate molecule to two specific Rab proteins, 1A and 3A (Seabra et al., 1992b). The enzyme itself is a multicomplex

composed of two components. The catalytic component, or component B is a heterodimer consisting of two subunits: a 60 kDa α-subunit and a 38 kDa β-subunit, both of which show sequence similarity to their respective FT and GGT I subunits (Armstrong et al., 1993; Seabra et al., 1992b). The second component, or component A of Rab GGT has also been completely purified from rat brain, and determined to be a 95 kDa subunit (Seabra et al., 1992a). Unlike the CAAX prenyltransferases, the α and β subunits of Rab GGT (from this point on simply referred to as Rab GGT) alone cannot prenylate Rab proteins, and instead require the presence of component A. It is absolutely crucial for both of these components to be present and physically associated in order for efficient prenylation of Rab proteins to occur (Seabra et al., 1992a; Seabra et al., 1992b).

Rab Escort Protein (REP)

Component A, now referred to as Rab Escort Protein-1 (REP-1) (Andres et al., 1993b) has been completely characterized and based on protein similarity to the human CHM gene product, established as the protein which is deficient in CHM (Seabra et al., 1992a). This has been further confirmed by elegant studies displaying REP-1 functional deficiency in lymphoblast extracts taken from CHM patients, and rescue of GGT activity by the addition of purified rat REP-1 (Seabra et al., 1993b).

REP-1 associates with Rab proteins

The significance of REP-1 activity in normal biological function can be appreciated in the context of the entire process of Rab prenylation (Fig. 1-6). In order for proper geranylgeranylation of newly synthesized Rabs to occur, REP must first form a stable complex with the nascent Rab molecule (Seabra et al., 1992a; Seabra et al., 1992b;

Shen and Seabra, 1996). However, the cysteine-rich sequences found at the C-terminus of the Rab proteins are not sufficient alone to facilitate recognition by REP-1. Numerous experiments have shown that short peptides containing the Rab C-terminal CXC or CC motif do not serve as either substrates for geranylgeranylation, nor do they efficiently compete for binding in geranylgeranylation assays (Moores et al., 1991; Khosravi-Far et al., 1991; Horiuchi et al., 1991; Farnsworth et al., 1991; Farnsworth et al., 1991; Seabra et al., 1992b). Furthermore, when Rab C-terminal motifs are altered, REP-1 is still able to associate with the mutant Rabs, in competition with wild-type Rabs (Seabra et al., 1992a). Since the C-terminal sequences alone do not contain enough information for REP-1 binding and subsequent geranylgeranylation, one can conclude that there must exist upstream sequences which are necessary for REP-1 to establish proper contact with Rabs. Many possible Rab protein motifs have been suggested as possible requirements for REP-1/Rab interaction, such as the early N-terminal sequences, and a so called hypervariable region of the C-terminus (Beranger et al., 1994; Overmeyer et al., 1998; Johannes et al., 1996; Sanford et al., 1995a). It has also been suggested that a Rab domain which undergoes nucleotide dependent conformational change may play a role in interaction with REP, explaining the preference of REP-1 for interaction with Rab proteins in the GDP-state. It seems that either one or all of these proposed motifs could be involved in REP binding.

Geranylgeranyl addition

The α and β subunits are the actual catalytic components of the Rab GGT holoenzyme, but cannot recognize Rab proteins alone, instead recognizing the stable

REP-1-Rab complex. Once this has occurred, Rab GGT is able to catalyze the transfer of GG groups from GG pyrophosphate to Rab C-terminal cysteine residues. Rab proteins are di-geranylgeranylated (Shen and Seabra, 1996; Horiuchi et al., 1991; Farnsworth et al., 1991). Each addition of a GG group occurs independently (Shen and Seabra, 1996). It appears that once a Rab protein is mono-geranylgeranylated, it remains in an extremely stable complex with REP-1 which *in vitro* is resistant to dissociation with detergents (Shen and Seabra, 1996). This prevents the premature release of mono-geranylgeranylated Rab from REP-1, before the Rab protein can be completely di-geranylgeranylated. Even though Rab GGT is obviously needed to catalyze geranylgeranylation, it is not involved in this stable association. In the normal situation, it is unknown whether the Rab GGT heterodimer remains bound to the REP-1-Rab complex after the first geranylgeranylation reaction or whether it dissociates after each step of the reaction.

REP-1 as a molecular chaperone

After the process of GGation is complete, REP-1 remains stably bound to the newly diGG-Rab molecule, and alone is capable of delivering the modified Rab to the appropriate organelle membrane (Andres et al., 1993b; Seabra et al., 1992a; Alexandrov et al., 1994b). Once the Rab properly interacts with the membrane, REP-1 dissociates from the complex and is free to involve itself in the prenylation of additional unmodified Rabs. This has been confirmed by *in vitro* studies which show that Rab geranylgeranylation efficiency rises dramatically in the presence of detergents (Andres et al., 1993b), due to the ability of the detergent to break this stable REP-1-diGG-Rab complex, freeing up REP for subsequent rounds of

geranylgeranylation. Whether there exists a Rab protein acceptor on the membrane surface responsible for dissociation of this REP-1-Rab interaction is still unknown. With the newly synthesized prenylated Rab stably associated in the organelle compartment membrane, the Rab cycle can now take place.

REP-1 and Rab GDI are similar in structure and function

Rab GDI shows sequence homology to REP-1 (Schalk et al., 1998; Waldherr et al., 1993; Fodor et al., 1991a; Andres et al., 1993a; Cremers et al., 1992a). Rab GDI also seems to functionally resemble REP-1, in that it preferentially binds to the GDP-bound Rab molecule (Ullrich et al., 1994a; Soldati et al., 1993; Alexandrov et al., 1994a) and can act as a molecular chaperone to prenylated Rab (Sanford et al., 1995b). In fact, it was this similarity between N-terminal regions of the REP-1 gene product and Rab GDI that initially led to the speculation that REP-1 interacted with Rab proteins (Fodor et al., 1991b; Cremers et al., 1992b; Seabra et al., 1992a). However, Rab GDI cannot assist in Rab geranylgeranylation (Alexandrov et al., 1994a), nor is it necessary for newly synthesized and geranylgeranylated Rabs to be delivered to membranes (Wilson et al., 1996). Although it has been shown that Rab GDI can readily accept newly geranylgeranylated Rabs and deliver them to membranes (Sanford et al., 1995b), consensus proposes that REP-1 ensures that Rabs are delivered to target membrane compartments immediately after Rab geranylgeranylation. The role of Rab GDI is to ensure multiple rounds of vesicular transport by recycling Rabs between cytosol and membrane after the first vesicular transport fusion event has occurred (Desnoyers et al., 1996; Alexandrov et al., 1994a; Novick and Zerial, 1997a; Wilson et al., 1996).

REP-1 vs REP-2

REP-1 is expressed ubiquitously, as shown in Northern blot studies (Cremers et al., 1990a) and Western analysis of rat tissues (Desnoyers et al., 1996). Therefore, it seems puzzling that CHM is a disorder that only affects eye-related tissues. The discovery of REP-2, a homologue of the CHM/REP-1 gene (Cremers et al., 1992a; Cremers et al., 1994), addresses this issue. REP-2 allows prenylation of most Rab proteins as efficiently as REP-1, which explains why CHM is not a disorder resulting in widespread cellular death in all tissues (Cremers et al., 1994). However, one specific Rab protein, Rab27 shows marked decreased geranylgeranylation in the presence of REP-2 as compared to REP-1 in CHM lymphoblasts (Seabra et al., 1995). Furthermore, Rab27 shows prominent expression in retinal tissues, particularly in the retinal pigment epithelium and choriocapillaris, two sites which are primarily affected early on in the disorder. Taken together, these results suggest that REP-2 is able to provide functional redundancy of REP-1 activity in all other tissues besides the RPE and choriocapillaris, unable to fully compensate for REP-1 activity with respect to Rab27. This creates a situation where the majority of Rab27 protein remains cytosolic and inactive, rendering them unable to mediate an undetermined aspect of vesicular transport in the RPE/choriocapillaris. It is important to note that in the absence of REP-1, REP-2 can still allow GGation of Rab27 at low efficiency (Seabra et al., 1995). CHM lymphoblast extracts also displayed some detectable Rab GGT residual activity which was dependent on the specific Rab protein used in determining geranylgeranylation efficiency, and this was presumably attributed to underlying REP-2 function (Seabra et al., 1993a). It has been postulated that this residual

geranylgeranylation of Rab27 by REP-2 could account for the slow loss of normal function in CHM eyes (Seabra, 1996). Initially at an early age, this low level Rab27 geranylgeranylation may be sufficient to maintain some homeostasis of retinal tissues. Once a minimum threshold of REP function is reached, a few cells begin to die, other cells in close proximity are then placed under additional stress, leading to subsequent widespread degeneration of the RPE, choriocapillaris and ultimately the entire retina.

In the current study, we have established a biochemical test based on immunological detection of the REP-1 protein in those suspected to have CHM. We have taken advantage of sufficient REP-1 expression in lymphocytes and the fact that that to date, only mutations which prematurely truncate the REP-1 gene product have been identified in CHM patients. In cases where the diagnosis has been confirmed, mutation detection has been utilized to identify specific familial mutations and alterations in the CHM gene. We believe that the initial step in the investigation of families where CHM has been clinically diagnosed is an immunological test, that provides a rapid and practical confirmation of the clinical diagnosis. Once CHM is confirmed, it is then possible to go on further with molecular genetic analysis to characterize the specific mutation in the individual, allowing for predictive and prenatal testing to potential carriers.

Materials and Methods

Families

Blood samples and pedigrees were obtained with informed consent from families with the initial diagnosis of CHM. Five families were ascertained through the practice of Dr. Ian MacDonald, Edmonton,Alberta (Family 1, 5) and upon referral from Dr. Richard Lewis, Houston, Texas (Family 2, 3) and Dr. Mandi Conway, New Orleans, Louisiana (Family 4).

Family 1

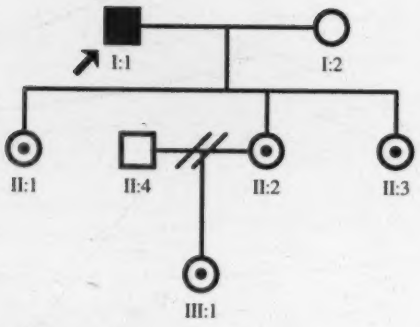

Family members tested		
Individual	Initials	CHM status
I:1	AP	affected
I:2	SP	normal
II:2	MP	carrier
III:1	HB	carrier

Clinical profile of proband

Affected individual I:1 was initially diagnosed with choroideremia at the age of 44 years, as a variant of retinitis pigmentosa. At the age of 67, his visual acuity was 20/70 OD and counting fingers OS. Slit lamp examination showed multiple "snowflake" opacities throughout the lens, and an anterior subcapsular cataract OS. Maximal visual fields were <5 degrees OU. Only a tiny residual island of washed out retina/RPE remained in the center of the fovea OU.

Family 2

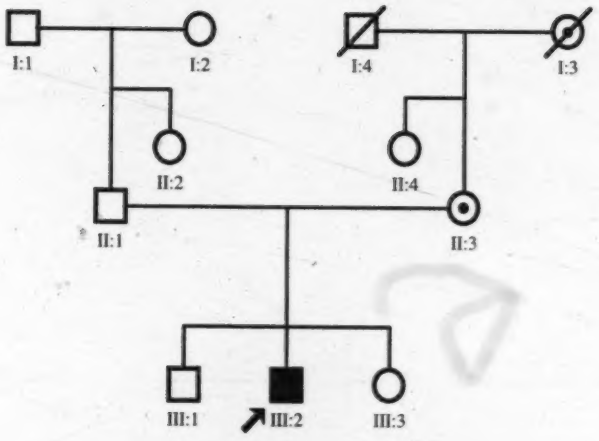

Family members tested		
Individual	Initials	CHM status
II:3	PB	carrier
III:2	JB	affected

Clinical profile of proband

Affected individual III:2 was initially diagnosed with CHM at the age of 23, with a history of poor peripheral vision since childhood. Confrontation visual fields showed concentric constriction to less than 20 degrees OU. Corrected vision was 20/20 OU. Examination of the mother (II:3) showed characteristic carrier changes in each fundus.

Family 3

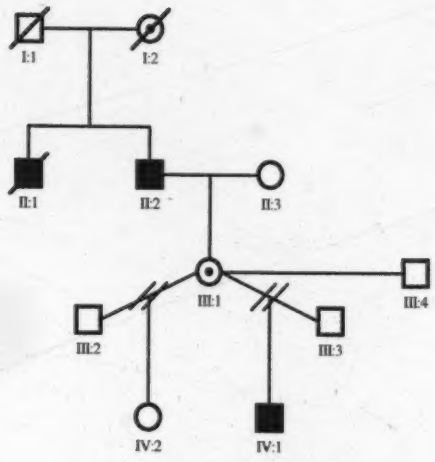

Family members tested		
Individual	Initials	CHM status
III:4	RC	normal
III:1	IC	carrier
IV:1	TC	affected

Clinical profile of affected individual tested

IV:1 presented at age 7 with a family history of choroideremia in his maternal grandfather and great uncle. At that time, his 32 year old mother was documented as an obligate carrier, both by her family history and fundus examination, which showed significant RPE changes in the periphery with an island of salt and pepper pigmentation in the macula. Corrected visual acuity of IV:1 was 20/25.

Family 4

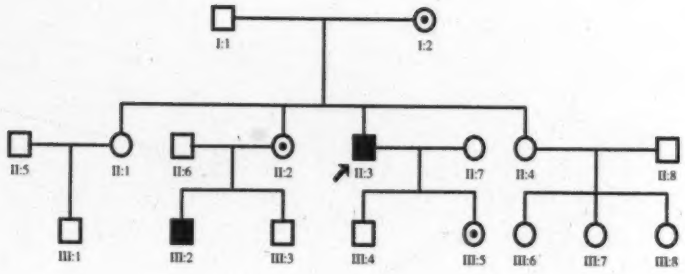

Family members tested		
Individual	Initials	CHM status
II:3	JG	affected
II:4	WH	normal
III:1	LA	normal
III:2	GM	affected
III:5	JM	carrier

Clinical profile of proband

II:3 was examined by Dr. Mandi Conway of the LSU Eye Center, New Orleans. He was described as having typical clinical fundus features of choroideremia. No further information was made available.

Family 5

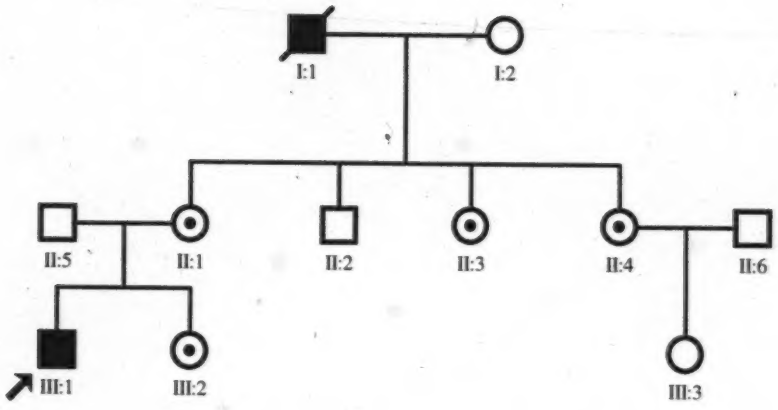

Family members tested		
Individual	Initials	CHM status
I:1	JS	affected
II:3	ES	carrier
II:4	BS	carrier
III:1	KR	affected

Clinical profile of proband

Despite significant peripheral chorioretinal atrophy, affected individual III:1 had no complaints of night blindness. When seen at age 21, corrected visual acuity was 20/20 OU. No formal visual field testing was performed. Fundus examination showed typical pattern of chorioretinal atrophy with sparing of central macula. Photograph of left fundus was obtained at age 17 (Fig. 1-2).

B95-8 cell line maintenance and Epstein-Barr Virus (EBV) production

The B95-8 cell line is a permanent cell line which releases high titers of transforming EBV (American Type Culture Collection, CRL 1612). This cell line was first established by transformation of marmoset blood leukocytes with EBV extracted from human leukocytes. The B95-8 cell line was initiated in 5 ml (Dulbecco's Modified Eagle Medium (D-MEM) media (Gibco-BRL) supplemented with 17% fetal calf serum and maintained in the same conditions at 37°C in a CO_2 incubator. The cell culture was subsequently incubated at 32°C for 1 week, allowing virus to be shed from the cell line. The cell solution was transferred to a 15 ml conical tube and centrifuged at 1000 g for 10 min. The supernatant was collected and syringe filtered through a 0.45 µl sterilizing filter. Appropriate dilutions of the EBV virus were made, and stored at –70°C.

Creation of lymphoblastoid cell lines

Patient and normal cell lines were created by EBV transformation of B-lymphocytes according to methods previously described (Anderson and Gusella, 1994) and modified by Dr. Ian M. MacDonald. Approximately 8 ml of peripheral blood taken from CHM patients and normals was collected in vials containing sodium heparin or lithium heparin and centrifuged at 1100 g for 30 min. The resulting layer containing the white blood cells was separated from plasma and the red blood cell layer, and subjected to white blood cell (WBC) extraction with Ficoll-Histopaque (Pharmacia-Biotech). WBC's were collected by centrifugation, and the WBC pellet was resuspended in 0.5 ml of RPMI 1640 media supplemented with 17% FCS (Gibco-BRL), 0.1% L-glutamine and 0.1% penicillin/streptomycin (Gibco-BRL). To this, 0.2

ml of EBV virus (1:1000 dilution) was added. The cell suspension was incubated for 2.5 h, at 37°C in 5% CO_2. Eight milliliters of media was added to the cell suspension. The entire cell mixture was transferred to T25 tissue culture flasks and again incubated at 37°C in CO_2 conditions. After 36-48 h, cells were washed with fresh media. Cells were incubated for approximately 1 week at 37°C in CO_2 conditions, and then observed for cell clumping and protruding pseudopodia, indicating successful transformation. Transformed cell lines were maintained in the same media as used above.

Protein extraction

Fifteen to twenty ml of peripheral blood taken from CHM patients and normals was collected in vials containing sodium heparin or lithium heparin and centrifuged at 1100 g for 30 min. The buffy coat layer was extracted and subjected to WBC extraction with Ficoll-Histopaque. Protein was also extracted from lymphoblastoid cells. WBC's and lymphoblastoid cells were collected by centrifugation and washed twice with phosphate-buffered saline (PBS). Cell lysates were prepared by homogenizing the cell pellets in an equal volume of cocktail containing 50 mM HEPES pH 7.2, 10 mM NaCl, 1 mM dithiothreitol, 1 mM Nonidet P-40, and protease inhibitors (5 µg/ml aprotinin, 5 µg/ml pepstatin, 5 µg/ml leupeptin and 0.5 mM phenylmethylsulfonylfluoride). Cell debris was precipitated by centrifugation at 100,000g for 1 h at 4°C. The supernatant protein concentration was determined with the Bradford Assay (Bio-Rad). Preliminary experiments determined that REP-1 was undetectable in red blood cells (RBC), therefore all protein analysis was restricted to WBC's or lymphoblastoid cells.

Western Analysis

Five µl of loading buffer (New England Biolabs (NEB)), and 1µl β-mercaptoethanol was added to 15 µl of protein sample (10-75 µg). Total protein was electrophoresed on a 7% sodium dodecyl sulphate (SDS)-polyacrylamide gel following the manufacturer's protocol (Bio-Rad Mini-PROTEAN® II Electrophoresis cell). Prestained protein markers (NEB) were used to monitor protein migration. Recombinant rat REP-1 protein was used as a positive control. Protein was electrotransferred (Bio-Rad Mini Trans-Blot® Electrophoretic transfer cell) as per the manufacturer's instructions to polyvinylidene difluoride membrane (Bio-Rad). The membrane was stained with Ponceau S (Sigma) to confirm adequate protein transfer. The remaining steps for Western analysis were as described elsewhere, and slightly altered to obtain optimal results (Gallagher et al., 1997). Membranes were blocked by incubation in PBS with 0.1% Tween 20 and 3% non-fat dry milk for 1 h at room temperature. Immunoblot analysis was done with 2 monoclonal antibodies: 2F1 (anti-REP-1 which recognizes the middle 210-420 amino acid epitope of the 653 amino acid protein, 1 µg/ml) and 1B7 (anti-α-subunit of farnesyl transferase (FTase), 1 µg /ml). FTase is a cytosolic enzyme which served as an internal control confirming adequate protein was loaded and detecting any evidence of proteolysis. For membranes containing protein extracted from WBC's, incubation was done with a 1:500 dilution of antibody for 2 h. Membranes containing lymphoblastoid cell protein were incubated for 1 h with antibody diluted to 1:1000. Membranes were washed for 30 min in 3 changes of PBS with 0.1% Tween 20, and incubated at room temperature with secondary anti-mouse IgG conjugated to horseradish peroxidase (Pierce,

1:25,000). After a final wash of 30 min with 3 changes of PBS with 0.1% Tween 20, antibody staining was detected by chemiluminescent detection (Luminol detection kit, Pierce) and exposure to autoradiographic film (Kodak X-OMAT).

DNA extraction from peripheral blood

Eight ml of peripheral blood from CHM patients and normal individuals was collected in vials containing ethylenediaminetetra-acetic acid (EDTA). The blood was centrifuged at 1000 g for 30 min, and the buffy coat layer was separated from plasma and RBC's. Lysate preparation, DNA extraction and precipitation were done according to methods previously described by Madisen and coworkers (1987). The buffy coat layer was mixed with 5 volumes of warm RBC lysis buffer (0.155 M NH_4Cl, 0.17 M TRIS, pH 7.65) and incubated at 37°C for 5 min, allowing the erythrocytes to lyse. WBC's were then collected by centrifugation at 1000 g for 10 min, and washed twice with NaCl solution (0.15 M). The WBC pellet was resuspended in 2 ml of high Tris-EDTA (TE) buffer (100 mM TRIS, 40 mM EDTA, pH 8.0) and immediately lysed with 2 ml of lysis mixture (0.2 % SDS, 1 M NaCl, 40 mM EDTA, 100 mM TRIS, pH 8.0) with vigorous mixing. The solution was extracted twice with an equal volume of TE-saturated phenol and once with an equal volume of chloroform:isoamyl alcohol (24:1). During these steps, aqueous and organic layers were separated by centrifugation at 1000 g for 10 min. DNA was precipitated by the addition of 1/10 volume of ammonium acetate (4 M) and an equal volume of isopropanol. The solution was mixed well and precipitated DNA was collected by spooling DNA strands with a plastic pipette tip. DNA was washed with 70% ethanol, air-dried and resuspended in 50-100 µl ddH_20 by continous overnight

rotation at 4°C. DNA was diluted with ddH_20 to a concentration of 5 ng/µl for PCR amplification and single stranded conformation polymorphism (SSCP) analysis. Samples were stored at 4°C.

Single-stranded conformation polymorphism (SSCP)

SSCP analysis was carried out according to methods described previously (Orita et al., 1989; Warren et al., 1997). Each exon of the CHM gene was amplified from genomic DNA with primer pairs (Research Genetics, Huntsville, AL) using annealing conditions reported previously by van Bokhoven and coworkers (Table 2-1) (1994a). PCR amplification was carried out randomly incorporating ^{35}S radiolabelled dATP directly into the PCR product, as described by Mirzayans and colleagues (1995). After an initial 5 min denaturation step at 95°C, 35 reaction cycles were performed as follows: 95°C for 30 sec, 30 sec at the appropriate annealing temperature, 72°C for 1 min. Final extension was carried out at 72°C for 10 min. PCR reactions contained 50 ng genomic template DNA, 60 ng each of forward and reverse primers, 200µM each of dGTP, dTTP, dCTP, 25 µm dATP, 5 µCi ^{35}S-dATP, 1 unit of *Thermus aquaticus* (Taq) polymerase (Sigma), 1X PCR buffer (Sigma 10X: 100mM TRIS, 500 mM KCl, 15 mM $MgCl_2$, 0.01% gelatin) and 0.8 µg/µl bovine serum albumin (BSA) in a final volume of 25 µl. Each reaction was overlayed with mineral oil to prevent evaporation during PCR. Following PCR amplification, 15 µl of stop solution (95% formamide, 10 mM NaOH, 0.05% bromophenol blue, 0.05% xylene cyanol) was added to the entire PCR reaction, denatured at 95°C for 5 min and cooled on ice. Five µl of each reaction was loaded and electrophoresed at 4°C on a 6% non-denaturing SSCP gel at 60 W for 5-6 h, in 1X Tris-borate/EDTA (TBE) buffer. For family 4, electrophoresis

was done at 6 W for 24 hr at room temperature, in order to better visualize the band shifts. Gels were dried under vacuum at 80°C and exposed to autoradiographic film (BioMax) for 24-36 hr.

Direct DNA sequencing

Where a mobility shift was detected in a specific exon, the exon was PCR amplified in conditions identical to those described above, excluding random incorporation of ^{35}S-dATP into the PCR product. The entire sample was mixed with 10 µl of loading buffer (0.3% Orange G, 20% Ficoll, 0.05% EDTA) and electrophoresed on a 1% agarose gel containing 0.7 µg/ml ethidium bromide. PCR fragments were excised from the agarose, and DNA was extracted and purified using the Quiaquick extraction kit (Qiagen) according to the manufacturer's protocol, and resuspended in 20 µl of ddH_2O. Direct sequencing was carried out with the ^{33}P-Thermosequenase kit (Amersham-Life Science) using appropriate CHM exonic primers as the forward and reverse sequence primers. Four µl of stop solution was added to 7 µl of PCR product, denatured at 95°C for 5 min and cooled on ice. Five µl was loaded on a 6% denaturing polyacrylamide gel and electrophoresed at 50 W for 1-2 h at room temperature, in 1X glycerol tolerant buffer (GTB) buffer. Gels were dried at 80°C under vacuum, and then exposed to autoradiography film (Biomax) for 8-12 h.

RNA isolation and reverse transriptase (RT) PCR

Total RNA was isolated from EBV-transformed cell lines with TRIZOL™ reagent (Gibco-BRL), according to manufacturer's instructions. In order to ensure adequate RNA and minimal RNA degradation, 1 µl of sample was electrophoresed on a 1.2% agarose gel containing 1X 3-(N-morpholino) propane-sulfonic acid (MOPS) buffer

and 0.66 M formaldehyde. Prior to RT, total RNA was treated with 10 units of RNase-free DNase I (Boehringer-Mannheim) at 37°C for 1 h to prevent genomic contamination. DNase I activity was inactivated by incubation at 70°C for 10 min. First-strand cDNA was synthesized with Superscript II RT (Gibco-BRL) using 100 ng of oligo-dT primer and 1 µg of total RNA. Incubation temperature and time was modified from the Superscript II RT protocol to 42°C for 45 min, and the reaction was terminated at 95°C for 5 min. A 1/250 dilution of the reverse transcribed cDNA was made. Five µl was subjected to PCR amplification with Taq polymerase, using primers constructed to span the putative deletion region: (primer 281: 5'-AAGCCAT TGCTCTTAGCAGG-3', primer 1346: 5'-AAGTAACTGTCCTCCACGAGG-3'). After denaturation at 95°C for 5 min, samples were amplified for 35 cycles: 30 sec at 95°C, 30 sec at 52°C and 1 min at 72°C. Following this, a final extension step was carried out at 72 °C for 10 min. PCR reactions contained template cDNA, 60 ng each of primers 281 and 1346, 200µm each of dGTP, dATP, dTTP, dCTP, 1 unit of Taq polymerase, 1X PCR buffer, 0.8 µg/µl BSA in a final volume of 25 µl. The entire sample was mixed with 10 µl loading buffer and electrophoresed on a 1% agarose gel containg 0.7 µg/ml ethidium bromide. PCR fragments were excised from the agarose and DNA was extracted and purified using the Qiaquick extraction kit, according to the manufacturer's protocol, and resuspended in 20 µl of ddH_20.

Sequence analysis of RT-PCR products

Direct sequencing of RT-PCR products was done as previously described above for exonic sequence, using primer 281 as the sequence primer.

Results

Western analysis

Western analysis was carried out to confirm the clinical diagnosis of CHM in affected males. Protein extracted from lymphocytes (Family 1, 4 or 5) or lymphoblastoid cell lines (Family 2 and 3) was subjected to immunoblot analysis with a highly specific REP-1 monoclonal antibody. Serial dilutions of protein extracted from WBC lysates taken from a normal male and female established the range of total protein at which the REP-1 protein could be detected (Fig. 3-1). Since all mutations to date have resulted in the premature truncation of the REP-1 gene product, we expected to see the absence of the REP-1 protein in those individuals affected with CHM.

Family 1

Western analysis performed on affected individual I:1 demonstrated that the REP-1 protein was indeed absent from protein extracted from his lymphocytes (Fig. 3-2), thereby confirming the clinical diagnosis of CHM. Other affected individuals were also shown to lack the REP-1 protein. As expected, REP-1 was detected in normal individuals.

Family 2

Western analysis performed on protein extracted from lymphoblastoid cell lines clearly showed that REP-1 was absent in affected individual III:2 (Fig. 3-3). Interestingly, his mother II:3 who is a carrier, also did not display any REP-1 protein. Recombinant rat REP-1 protein used as a positive control migrated somewhat slower than that of human REP-1 protein, due to its slight dissimilarity in amino acid sequence compared to human REP-1.

Family 3

Lymphoblastoid protein taken from affected individual IV:1 lacked any evidence of REP-1 product when subjected to Western analysis (Fig. 3-4). His mother III:1, a female carrier, displayed detectable, albeit a lesser amount, REP-1 protein compared to that of the normal control.

Family 4

Western analysis showed that the affected individual in this family, II:3, displayed no detectable REP-1 protein in his lymphocyte protein sample (Fig. 3-5). His carrier daughter III:5 did show normal levels of REP-1 product.

Family 5

Protein extracted from lymphocytes taken from III:1 demonstrated that REP-1 product was absent (Fig. 3-6). This was also shown for another affected individual. Both carrier females and normal individuals displayed normal levels of REP-1 protein.

SSCP analysis

In order to localize the position of the specific mutation in the CHM gene in each family, every one of the 15 CHM exons was PCR-amplified separately from DNA extracted from lymphocytes, and subject to SSCP analysis. If a polymorphism was revealed, its segregation was tested for. In all cases presented here, the results suggested the presence of a polymorphism that segregated with the disease in the family. Primer pairs and PCR conditions used for each exon were previously described (Table 2-1).

Family 1

A band shift was detected in individual I:1 for the PCR fragment corresponding to the entire sequence of exon 7 (Fig. 3-7). A heterozygous banding pattern was also shown in his daughter II:2 and granddaughter III:1, confirming their carrier status. No band shift was observed for the normal female I:2, or seen in the other PCR-amplified exons (data not shown).

Family 2

SSCP analysis of the second half of exon 5 (exon 5b) revealed a band shift in individual III:2 (Fig. 3-8). His mother II:3 displayed a heterozygous banding pattern, while the normal individual showed no detectable band shift.

Family 3

A band shift in exon 6 was detected in individual IV:1 (Fig.3-9). His father III:4 displayed the normal banding pattern, while his mother III:1 showed the heterozygous banding pattern typical of a female carrier.

Family 4

SSCP analysis of exon 1 from this family detected a band shift in individuals II:3 and III:2 (Fig. 3-10). In the female carrier III:5, the characteristic heterozygous banding pattern was evident. Normal individuals II:4 and III:1 showed no band shift.

DNA sequence analysis

Direct cycle-sequencing of the gel-shifted PCR product was carried out using the appropriate exonic primers as sequencing primers for the sequencing reaction. By doing so, we established direct proof that the clinical diagnosis was the direct result of specific mutations in the CHM gene, in order to corroborate our western studies.

Family 1

Sequencing of the gel-shifted PCR product of exon 7 in individual I:1 revealed a cytosine to thymine transition mutation at position 907 of the coding region of the CHM gene (Fig. 3-11). This base alteration results in a TGA stop codon at the usual arginine residue at amino acid position 293, leading to the premature truncation of the protein. Individual II:2 was seen to be heterozygous for this mutation.

Family 2

Exon 5b was sequenced in individual III:2 which revealed a 2 base adenine-guanine deletion at position 555/556 (Fig. 3-12). The deletion results in a frameshift, and the introduction of a stop codon 18 bases downstream.

Family 3

Sequence analysis of exon 6 in individual IV:1 demonstrated the presence of a cytosine to thymine transition mutation at position 787 (Fig. 3-13). This base alteration introduces a TGA stop codon at the normal arginine residue found at amino acid position 253. Individual III:1 showed heterozygosity at this position.

Family 4

Exon 1 sequencing revealed a single cytosine deletion at position 45 in individual II:3 (Fig. 3-14). This frameshift leads to the introduction of a stop codon approximately 15 bases downstream of this deletion. Individual III:5, a female expected to be heterozygous for the CHM mutation, showed a one base misalignment of sequence occurring immediately after this single base deletion. This indicates that this deletion is present in only a single CHM gene copy.

RT-PCR

In family 5, repeated attempts to PCR-amplify exons 5 to 8 from genomic DNA from the affected members I:1 and III:1 were unsuccessful (Fig. 3-15). Therefore, to test the possibility of an intragenic deletion, exonic PCR primers were designed to flank the putative deletion junction (Fig. 3-16a). As PCR size constraints would not allow us to amplify across this region from genomic DNA, expected to be up to 24 kb, these primers were used to amplify across the deletion junction in mRNA extracted from individual III:1 and a normal control. The presence of a smaller sized band in III:1 is clearly evident (Fig. 3-16b). This band is approximately 900 bases smaller than that seen in the normal control, closely corresponding to the amount of mRNA sequence which should be absent from the complete deletion of exons 5 to 8. This result confirms the deletion in individual III:1.

Direct sequencing of the RT-PCR product

Direct sequencing of the smaller band from individual III:1 confirmed the absence of exons 5 to 8 in the mRNA product (Fig. 3-17). Therefore, we assume that the deletion of genomic DNA in individual III:1 encompasses at least exons 5 through 8, including intervening intronic sequence, and that the transcribed mRNA molecule is spliced directly from exon 4 to exon 9.

This resulting mRNA molecule, although still entirely in frame, encodes a truncated protein missing approximately one-third of its amino acid sequence. Unfortunately, the polypeptide sequence which is deleted corresponds to almost the entire epitope to which the REP-1 monoclonal antibody recognizes. Immunoblot analysis to detect the

truncated protein with a polyclonal REP-1 antibody have so far been unsuccessful (data not shown). We attribute this to the likelihood that this truncated REP-1 gene product, although presumably containing both normal C-terminal and N-terminal domains, would suffer from a loss of such a significant portion of protein and be unable to adopt the proper protein conformation. The cell would then rapidly degrade this aberrant REP-1 polypeptide, which would not be detected by immunoblot analysis with any mono- or polyclonal antibody.

Discussion

We have utilized an immunological based test to biochemically determine the clinical status of affected males and female carriers in five families suspected to have CHM. Two factors which have enabled us to perform this task are REP-1 expression in lymphocytes and the presence of only mutations in the REP-1 gene which truncate the gene product. Protein from individuals was extracted from lymphocytes or lymphoblast cell lines, and subjected to REP-1 detection with a monoclonal antibody. Every affected individual tested from the five different families displayed no detectable levels of REP-1 protein, thereby confirming the validity and reliability of immunoblot analysis as a diagnostic test. Once the diagnosis could be attributed to absence of REP-1 protein, mutation analysis was carried out to locate specific defects in the REP-1 gene. SSCP analysis was initially used to localize the mutation to a specific exon, followed by direct sequencing which allowed for characterization of the specific mutation. In addition, RT-PCR analysis and direct sequencing was used to characterize an intragenic microdeletion discovered in one family. In total, two transition mutations, two small nucleotide deletions and one large deletion encompassing four exons were identified in the CHM gene.

Described Mutations

Recently, we and many other groups have worked to identify mutations within the REP-1 gene (van den Hurk et al., 1992; van den Hurk et al., 1997b; van Bokhoven et al., 1994a) (Beaufrere et al., 1996; Forsythe et al., 1997; Nesslinger et al., 1996). All five mutations described in this study are similar to those seen previously in the literature (Table 4-1). Mutations described in this research are not localized to one

particular region of the REP-1 gene, as is the case with other previously described mutations which are scattered across the entire gene (Fig. 4-1). Two mutations presented here, an AG deletion in exon 5 and a C→T transition mutation in exon 7 are identical to mutations reported previously (van Bokhoven et al., 1994a). Whether these mutations originate from the same founder or represent a common mutational site has yet to be determined. The other three mutations described here are unique and have not been reported before.

The mutations presented in this study all result in premature truncation during translation. To date, only protein-truncating mutations have ever been found.[1] Why has there been no confirmed case of a missense mutation in the REP-1 gene? There may be a number of possible explanations for this. A missense mutation may result in a partially functional REP-1 gene product, depending on its location within the gene. If this is the case, it could result in a milder phenotype which would not be detected clinically. However, a missense mutation which rendered REP-1 unable to chaperone Rab, but still allowed Rab protein binding, or one which resulted in irreversible REP-1-Rab binding could have more serious consequences than a null mutation. With the aberrant REP-1 protein still able to form a stable complex with Rab, it would competitively inhibit binding by REP-2 or possibly other members of a REP family. In such a scenario, even compensatory Rab geranylgeranylation could not occur in other tissues besides the eye. Such a serious defect could result in embryonic lethality, and manifest as a stillborn birth or spontaneous abortion. In either case, an

[1] A missense mutation has been reported previously (Donnelly et al., 1994), but subsequent work has shown that it is actually a splice site alteraction (Beaufrere, 1998).

ascertainment bias would exist against the discovery of missense mutations in the REP-1 gene.

The fact that no missense mutations have been identified, makes it difficult to assign functional significance to specific protein domains. However, these mutations that are described here, in addition to those previously reported, do comment on the functional stability of the REP-1 gene product. No correlation is seen between the position of the truncating mutation and the resulting clinical phenotype. This suggests that if the entire coding region is not translated, the protein is unstable and presumably degraded by the cell. This notion is further supported by our finding of an intragenic deletion in the CHM gene, which produces an in-frame protein product. This truncated protein, with the middle third portion absent and containing its proper N- and C-termini, is not detected by immunoblot analysis. Thus, the deletion of even a middle portion of the protein presumably upsets proper protein conformation and stability within the cell.

Future work

Continued mutation detection

The continued search for mutations in the REP-1 gene which result in CHM will be essential in increasing our knowledge regarding REP-1 function and the CHM disease process. Obviously, it will be of great interest if and when a confirmed missense mutation is found within the REP-1 gene. Such a discovery will help identify domains necessary for Rab protein or Rab GGT interaction. Once the REP-1 promoter region is fully characterized, it will also serve as another region of interest for mutation detection. Identifying promoter mutations will provide insight into how REP-1 expression is controlled and what factors are involved. The identification of such

factors may help explain any phenotypic variability seen between affected individuals. Finally, as more mutations are found which truncate the REP-1 gene product, common mutations and mutational hotspots may be discovered, which could contribute to future studies analyzing REP-1 function, and provide valuable information to those families carrying such mutations.

X-inactivation of the REP-1 gene

As females have two X-chromosomes while males have only one, females possess twice the amount of X-chromosomal genetic information as males do. In order to compensate for this extra dosage, one X-chromosome is randomly condensed in female somatic cells, and rendered inactive. Some preliminary data suggests that the CHM gene may in fact escape this X-inactivation (Carrel and Willard, 1996; Carrel and Willard, 1993). Interestingly, our Western results show the absence of REP-1 protein in a carrier female from Family 2. This may be a clonal artifact of the EBV transformation procedure, where an entire population of cells may represent a few that have had the normal gene product inactivated. On the other hand, this may represent skewed inactivation of the normal gene product in this individual. However, this seems unlikely since the female exhibits only carrier signs and does not manifest the changes seen in a CHM male. In any case, this finding suggests that the CHM gene does not escape X-inactivation. Random X-inactivation of the CHM gene would correlate well with the clinical signs seen in the female carrier. Patchy areas of RPE cells with irregular pigmentation and morphology could be attributed to the proliferation of a clonal cell population derived from a few cells with the REP-1 gene inactivated. The fact that only isolated populations of the defective cells exist in the

female carrier, would explain why the full clinical onset of CHM does not occur. Current X-inactivation studies are underway in order to confirm whether this is indeed the case.

A REP protein family?

It seems only natural to assume that a family of REP proteins may exist, which could handle prenylation of such a large and diverse family of Rab proteins. The fact that some Rab proteins seem to be more efficiently geranylgeranylated by one REP or the other makes it seem highly possible that specific REPs are responsible for binding different Rab proteins. Indeed, in Western results presented here (Fig. 3.3, 3.4 and 3.5) and immunoblot analysis done under less stringent conditions, REP-1 monoclonal antibody identifies extra products which presumably represent other REP isoforms (data not shown). The identification of other members of the REP protein family will provide a clearer understanding of the specific factors involved in vesicular transport within different compartments of the cell, and between different cell types.

Mutations in GDI : A GDI protein family?

CHM is a unique disorder with respect to the underlying biochemical defect responsible for its phenotype. No other known human disorder is caused by defects in prenylation and subsequent inactivity of nascent Rab proteins. However recently, mutations have been found in the Rab GDI gene, which may be responsible for some forms of X-linked mental retardation (DAdamo et al., 1998). As stated previously, Rab GDI is necessary for the recycling of Rab proteins during the Rab cycle, thereby ensuring multiple rounds of vesicular transport. In terms of studying CHM, this is quite a substantial finding, due to the structural and functional homology between

REP-1 and Rab GDI, and the functional relationship that exists between them in the Rab cycle. By studying a defect in this aspect of the Rab cycle leading to a phenotype distinct from CHM, more knowledge is gained regarding the Rab cycle and the complex nature of vesicular trafficking in general. Furthermore, the identification of a GDI responsible for mental retardation leads to the assumption that it may be brain specific and involved in neuronal development and maintenance. This suggests that a GDI family of proteins may exist, with specific members responsible for different components of cellular vesicular transport.

Animal models

Transgenic animal models are often established in order to achieve a greater understanding of the pathogenesis of a disease. Although no definite model for CHM has yet been created, preliminary work with a transgenic mouse model does give some insight into what features of the retina are primarily affected by REP-1 deficiency (van den Hurk et al., 1997a). In this model, the REP-1 gene mutation was not successfully transmitted through the maternal germline. The authors proposed that in mice, REP-1 activity is required for the survival of extraembryonic membranes. This would explain the embryonic lethality observed in hemizygous males offspring. The inability of female mice to pass the CHM gene to female offspring was attributed to preferential X-inactivation of the paternal X-chromosome in mice. Thus, with the wildtype paternal gene inactive, and only the mutant copy expressed on the maternal X-chromosome, female embryos would also not survive. Therefore, only reliable histopathological data could be obtained from chimeric male mice and female heterozygotes that inherited the CHM allele through the paternal germline.

Heterozygous female mice showed no obvious visual defects upon ERG examination and areas of mild photoreceptor loss. Conversely, chimeric male mice showed some retinal dysfunction and areas of complete photoreceptor degeneration. In both cases, it should be noted that the histopathological findings in both male and female mice showed loss of photoreceptors with normal and intact RPE and choroid. This possibly suggests a defect in intracellular transport within the photoreceptor cell. This data contradicts most other histopathological evidence showing initial atrophy of the RPE and choroid preceding secondary degeneration of the photoreceptors. More studies involving transgenic models will have to be done in order to establish a reliable mechanism for the degeneration process which occurs in CHM.

Gene therapy

Unfortunately, at the present time there exists no effective method to treat or even slow the progression of CHM. Our recent understanding of CHM as a biochemical disorder and the identification of the defective enzyme component responsible for CHM makes the disorder a good candidate for gene therapy. However, a major problem exists that prevents the pursuit of such therapy. It is still not known which tissues are primarily defective in CHM, nor what the consequences would be if REP-1 was non-specifically expressed in the CHM retina. This makes it extremely difficult to target a specific cell type for gene therapy. Inappropriate cell targeting could result in ineffective treatment, or possibly even detrimental effects to the patient. Only when the pathogenesis of CHM is sufficiently understood will it be possible to utilize gene therapy to treat this disorder.

Conclusion

The prevalence of choroideremia in Canada has not been published, but could be estimated as 1 in 325,000 by comparison with U.S. estimates (Lewis et al., 1985). The progressive nature of the disorder dictates that affected males and carrier females may not show clinical signs until later on in life, contributing to early uncertainty in diagnosis. Even when visual problems are attributed to peripheral retinal dysfunction, CHM may be overlooked as the diagnosis. The clinical signs of CHM resemble those seen in other eye-related disorders such as X-linked retinitis pigmentosa. However, the clinical prognoses for each of these is quite distinct, in that those afflicted with CHM usually maintain central visual acuity until quite late in the progression of the disease. Therefore, it is of great importance to be able to unequivocally determine the correct diagnosis and allow the affected families to know for certain what eye-related disorder they are affected with. Determining the correct diagnosis is also critical in ensuring that proper genetic counseling and long term patient care can be provided to affected families. The significance of such a confirmatory biochemical test for the clinical diagnosis of CHM is clearly evident.

We believe that the first step in investigating families suspected to have CHM is immunoblot analysis to determine the presence or absence of the REP-1 protein in suspected CHM individuals. The test described here is able to immediately confirm affected status in males clinically diagnosed with CHM. It is both reliable and efficient in terms of the actual procedure and achieving reproducible results. From a practical standpoint, it is less time consuming and less expensive compared to molecular genetic analysis of the REP-1 gene. However, because the test itself is

limited in that REP-1 protein detection is not a quantitative assay and cannot confirm carrier status in those suspected to be carriers, characterization of the disease-causing REP-1 gene mutation should be subsequently carried out. Once the mutation in the REP-1 gene is discovered, it makes it possible to test family members other than those that may be affected, and conduct prenatal and presymptomatic diagnosis. In the five families which we have studied, carrier status was confirmed in exactly such a manner. It is this sequential process that should be followed when studying families with CHM. The data presented here emphasizes the effectiveness and importance of this immunoblot analysis as a diagnostic tool alone, and when carried out in conjunction with molecular genetic analysis. By investigating CHM families in such a manner, invaluable information will be provided to those families affected with CHM.

Reference List

1. Alexandrov, K., Horiuchi, H., Steele-Mortimer, O., Seabra, M.C. and Zerial, M. Rab escort protein-1 is a multifunctional protein that accompanies newly prenylated rab proteins to their target membranes. *EMBO J.* 13:5262-5273, 1994a.

2. Anderson, M.E. and Gusella, J.F. Use of cyclosporin A in establishing Epstein-Barr virus-transformed human lymphoblastoid cell lines. *In Vitro* 20:856-858, 1994.

3. Andres, D.A., Seabra, M.C., Brown, M.S., et al. cDNA cloning of component A of Rab geranylgeranyl transferase and demonstration of its role as a Rab escort protein. *Cell* 73:1091-1099, 1993a.

4. Armstrong, S.A., Seabra, M.C., Sudhof, T.C., Goldstein, J.L. and Brown, M.S. cDNA cloning and expression of the α and β subunits of rat Rab Geranylgeranyltransferase. *J.Biol.Chem.* 268:12221-12229, 1993.

5. Beaufrere, L. No missense mutation in the choroideremia (CHM) gene. *Exp.Eye Res.* 1998.

6. Beaufrere, L., Tuffery, S., Hamel, C., Arnaud, B., Demaille, J. and Claustres, M. A novel mutation (S558X) causing choroideremia. *Hum.Mutat.* 8:3951996.

7. Beranger, F., Cadwallader, K., Porfiri, E., et al. Determination of structural requirements for the interaction of Rab6 with RabGDI and Rab geranylgeranyltransferase. *J.Biol.Chem.* 269:13637-13643, 1994.

8. Carr, R.E. and Noble, K.G. Disorders of the fundus. 2. Choroideremia. *Ophthalmology* 87:169-171, 1980.

9. Carrel, L. and Willard, H.F. The X-linked choroideremia gene escapes X chromosome activation. *Am.S.Hum.Genet.Annual Meeting* 1993.(Abstract)

10. Carrel, L. and Willard, H.F. The choroideremia gene escapes X inactivation in some females, but not in others: heterogeneity in control of gene expression from the inactive X. *Am.S.Hum.Genet.Annual Meeting* 1996.(Abstract)

11. Casey, P.J. and Seabra, M.C. Protein prenyltransferases. *J.Biol.Chem.* 271:5289-5292, 1996.

12. Clarke, S.J. Protein isoprenylation and methylation at carboxyl-terminal cysteine residues. *Annu.Rev.Biochem.* 61:355-386, 1992.

13. Cremers, F.P., Armstrong, S.A., Seabra, M.C., Brown, M.S. and Goldstein, J.L. REP-2, a Rab escort protein encoded by the choroideremia-like gene. *J.Biol.Chem.* 269:2111-2117, 1994.

14. Cremers, F.P., Molloy, C.M., van de Pol, D.J., et al. An autosomal homologue of the choroideremia gene colocalizes with the Usher syndrome type II locus on the distal part of chromosome 1q. *Hum.Mol.Genet.* 1:71-75, 1992a.

15. Cremers, F.P., Sankila, E.M., Brunsmann, F., et al. Deletions in patients with classical choroideremia vary in size from 45 kb to several megabases. *Am.J.Hum.Genet.* 47:622-628, 1990.

16. Cremers, F.P., van de Pol, D.J., Diergaarde, P.J., et al. Physical fine mapping of the choroideremia locus using Xq21 deletions associated with complex syndromes. *Genomics* 4:41-46, 1989.

17. Cremers, F.P., van de Pol, D.J., van Kerkhoff, L.P., Wieringa, B. and Ropers, H.H. Cloning of a gene that is rearranged in patients with choroideraemia [see comments]. *Nature* 347:674-677, 1990a.

18. Cremers, F.P., van de Pol, D.J., Wieringa, B., et al. Chromosomal jumping from the DXS165 locus allows molecular characterization of four microdeletions and a de novo chromosome X/13 translocation associated with choroideremia. *Proc.Natl.Acad.Sci.U.S.A.* 86:7510-7514, 1989.

19. DAdamo, P., Gulisano, M., Oostra, B.A., Chelly, J. and Toniolo, D. GDI is responsible for X-linked metal retardation. *Am.S.Hum.Genet.Annual Meeting* 1998.(Abstract)

20. Desnoyers, L., Anant, J.S. and Seabra, M.C. Geranylgeranylation of Rab proteins. *Biochem.Soc.Trans.* 24:699-703, 1996.

21. Dirac-Svejstrup, A.B., Sumizawa, T. and Pfeffer, S.R. Identification of a GDI displacement factor that releases endosomal Rab GTPases from Rab-GDI. *EMBO J.* 16:465-472, 1997.

22. Donnelly, P., Menet, H., Fouanon, C., et al. Missense mutation in the choroideremia gene. *Hum.Mol.Genet.* 3:10171994.

23. Epstein, W.W., Lever, D., Leining, L.M., Bruenger, E. and Rilling, H.C. Quantitation of prenylcysteines by a selective cleavage reaction. *Proc.Natl.Acad.Sci.U.S.A.* 88:9668-9670, 1991.

24. Farnsworth, C.C., Kawata, M., Yoshida, Y., Takai, Y., Gelb, M.H. and Glomset, J.A. C terminus of the small GTP-binding protein smg p25A contains two geranylgeranylated cysteine residues and a methyl ester. *Proc.Natl.Acad.Sci.U.S.A.* 88:6196-6200, 1991.

25. Flannery, J.G., Bird, A.C., Farber, D.B., Weleber, R.G. and Bok, D. A histopathologic study of a choroideremia carrier. *Invest.Ophthalmol.Vis.Sci.* 31:229-236, 1990.

26. Fodor, E., Lee, R.T. and O'Donnell, J.J. Analysis of choroideraemia gene [letter]. *Nature* 351:6141991a.

27. Forsius, H., Hyvarinen, L., Nieminen, H. and Flower, R. Fluorescein and indocyanine green fluorescence angiography in study of affected males and in female carriers with choroidermia. A preliminary report. *Acta Ophthalmol.(Copenh.)* 55:459-470, 1977.

28. Forsythe, P., Maguire, A., Fujita, R., Moen, C., Swaroop, A. and Bennett, J. A carboxy-terminal truncation of 99 amino acids resulting from a novel mutation (Arg555-->stop) in the CHM gene leads to choroideremia [letter]. *Exp.Eye Res.* 64:487-490, 1997.

29. Francois, J. Choroideremia (progressive chorioretinal degeneration). *Int.Ophthalmol.Clin.* 8:949-964, 1968.

30. Fraser, G.R. and Friedmann, A.I. Choroideremia in a female. *Br.Med.J.* 2:732-734, 1968.

31. Fukui, K., Sasaki, T., Imazumi, K., Matsuura, Y., Nakanashi, H. and Takai, Y. Isolation and characterization of a GTPase activating protein specific for the Rab3 subfamily of small G proteins. *J.Biol.Chem.* 272:4655-4658, 1997.

32. Gal, A., Brunsmann, F., Hogenkamp, D., et al. Choroideremia-locus maps between DXS3 and DXS11 on Xq. *Hum.Genet.* 73:123-126, 1986.

33. Gallagher, S., Winston, S.E., Fuller, S.A. and Hurrell, J.G.R. Analysis of Proteins. In: *Current Protocols in Molecular Biology* , edited by Ausubel, F.M., Brent, R., Kingston, R.E., et al. Massachusetts: John Wiley & Sons, Inc., 1997, p. 10.8.8-10.8.14

34. Ghosh, M. and McCulloch, J.C. Pathological findings from two cases of choroideremia. *Can.J.Ophthalmol.* 15:147-153, 1980.

35. Glomset, J.A. and Farnsworth, C.C. Role of protein modification reactions in programming interactions between Ras-related GTPases and cell membranes. *Annu.Rev.Cell.Biol.* 10:181-205, 1994.

36. Harris, G.S. and Miller, J.R. Choroideremia. Visual defects in a heterozygote. *Arch.Ophthalmol.* 80:423-429, 1968.

37. Hodgson, S.V., Robertson, M.E., Fear, C.N., et al. Prenatal diagnosis of X-linked choroideremia with mental retardation, associated with a cytologically detectable X-chromosome deletion. *Hum.Genet.* 75:286-290, 1987.

38. Horiuchi, H., Kawata, M., Kato, H., et al. A novel prenyltransferase for a small GTP-binding protein having a C-terminal Cys-Ala-Cys structure. *J.Biol.Chem.* 266:16981-16984, 1991.

39. Jay, M., Wright, A.F., Clayton, J.F., et al. A genetic linkage study of choroideremia. *Ophthalmic Paediatr.Genet.* 7:201-204, 1986.

40. Johannes, L., Perez, F., Laran-Chich, M.P., Henry, J.P. and Darchen, F. Characterization of the interaction of the monomeric GTP-binding protein Rab3a with geranylgeranyl transferase II. *Eur.J.Biochem.* 239:362-368, 1996.

41. Khosravi-Far, R., Lutz, R.J., Cox, A.D., et al. Isoprenoid modification of rab proteins terminating in CC or CXC motifs. *Proc.Natl.Acad.Sci.U.S.A.* 88:6264-6268, 1991.

42. Kinsella, B.T. and Maltese, W.A. rab GTP-binding proteins with three different carboxyl-terminal cysteine motifs are modified in vivo by 20-carbon isoprenoids. *J.Biol.Chem.* 267:3940-3945, 1992.

43. Kurstjens, J.M. Choroideremia and gyrate atrophy of the choroid and retina. *Documenta Ophthalmologica* 19:1-78, 1965.

44. Lesko, J.G., Lewis, R.A. and Nussbaum, R.L. Multipoint linkage analysis of loci in the proximal long arm of the human X chromosome: application to mapping the choroideremia locus. *Am.J.Hum.Genet.* 40:303-311, 1987.

45. Lewis, R.A., Nussbaum, R.L. and Ferrell, R. Mapping X-linked ophthalmic diseases. Provisional assignment of the locus for choroideremia to Xq13-q24. *Ophthalmology* 92:800-806, 1985.

46. MacDonald, I.M., Chen, M.H., Addison, D.J., Mielke, B.W. and Nesslinger, N.J. Histopathology of the retinal pigment epithelium of a female carrier of choroideremia. *Can.J.Ophthalmol.* 32:329-333, 1997.

47. MacDonald, I.M., Sandre, R.M., Wong, P., Hunter, A.G. and Tenniswood, M.P. Linkage relationships of X-linked choroideremia to DXYS1 and DXS3. *Hum.Genet.* 77:233-235, 1987.

48. Madisen, L., Hoar, D.I., Holroyd, C.D., Crisp, M. and Hodes, M.E. DNA banking: the effects of storage of blood and isolated DNA on the integrity of DNA. *Am.J.Med.Genet.* 27:379-390, 1987.

49. Matsui, Y., Kikuchi, A., Araki, S., et al. Molecular cloning and characterization of a novel type of regulatory protein (GDI) for smg p25A, a ras p21-like GTP-binding protein. *Mol.Cell Biol.* 10:4116-4122, 1990.

50. Mauthner. Ein Fall von Choroideremia. *Ber.d.naturw-med.Ver.in Inssbruck* 2:1911871.

51. McCulloch, C. and McCulloch, J.C. A hereditary and clinical study of choroideremia. *American Academy of Ophthalmology and Otolaryngology Transactions* 52:160-190, 1948.

52. Merry, D.E., Janne, P.A., Landers, J.E., Lewis, R.A. and Nussbaum, R.L. Isolation of a candidate gene for choroideremia. *Proc.Natl.Acad.Sci.U.S.A.* 89:2135-2139, 1992.

53. Merry, D.E., Lesko, J.G., Siu, V., et al. DXS165 detects a translocation breakpoint in a woman with choroideremia and a de novo X; 13 translocation. *Genomics* 6:609-615, 1990.

54. Merry, D.E., Lesko, J.G., Sosnoski, D.M., et al. Choroideremia and deafness with stapes fixation: a contiguous gene deletion syndrome in Xq21. *Am.J.Hum.Genet.* 45:530-540, 1989.

55. Mirzayans, F., Pearce, W.G., MacDonald, I.M. and Walter, M.A. Mutation of the PAX6 gene in patients with autosomal dominant keratitis. *Am.J.Hum.Genet.* 57:539-548, 1995.

56. Moores, S.L., Schaber, M.D., Mosser, S.D., et al. Sequence dependence of protein isoprenylation. *J.Biol.Chem.* 266:14603-14610, 1991.

57. Nesslinger, N., Mitchell, G., Strasberg, P. and MacDonald, I.M. Mutation analysis in Canadian families with choroideremia [see comments]. *Ophthalmic Genet.* 17:47-52, 1996.

58. Noble, K.G., Carr, R.E. and Siegel, I.M. Fluorescein angiography of the hereditary choroidal dystrophies. *Br.J.Ophthalmol.* 61:43-53, 1977.

59. Novick, P. and Brennwald, P. Friends and family: the role of the Rab GTPases in vesicular traffic. *Cell* 75:597-601, 1993.

60. Novick, P. and Zerial, M. The diversity of Rab proteins in vesicle transport. *Curr.Opin.Cell Biol.* 9:496-504, 1997a.

61. Nuoffer, C. and Balch, W.E. GTPases: multifunctional molecular switches regulating vesicular traffic. *Annu.Rev.Biochem.* 63:949-990, 1994.

62. Nussbaum, R.L., Lesko, J.G., Lewis, R.A., Ledbetter, S.A. and Ledbetter, D.H. Isolation of anonymous DNA sequences from within a submicroscopic X chromosomal deletion in a patient with choroideremia, deafness, and mental retardation. *Proc.Natl.Acad.Sci.U.S.A.* 84:6521-6525, 1987.

63. Nussbaum, R.L., Lewis, R.A., Lesko, J.G. and Ferrell, R. Choroideremia is linked to the restriction fragment length polymorphism DXYS1 at XQ13-21. *Am.J.Hum.Genet.* 37:473-481, 1985.

64. Orita, M., Suzuki, Y., Sekiya, T. and Hayashi, K. Rapid and sensitive detection of point mutations and DNA polymorphisms using the polymerase chain reaction. *Genomics* 5:874-879, 1989.

65. Overmeyer, J.H., Wilson, A.L., Erdman, R.A. and Maltese, W.A. The putative "switch 2" domain of the Ras-related GTPase, Rab1B, plays an essential role in the interaction with Rab escort protein. *Mol.Biol.Cell* 9:223-235, 1998.

66. Pameyer, J.K., Waardenburg, P.J. and Henkes, H.E. Choroideremia. *Br.J.Ophthalmol.* 44:724-738, 1960.

67. Pfeffer, S.R. Rab GTPases: master regulators of membrane trafficking. *Curr.Opin.Cell Biol.* 6:522-526, 1994.

68. Rafuse, E.V. and McCulloch, C. Choroideremia. A pathological report. *Can.J.Ophthalmol.* 3:347-352, 1968.

69. Rodrigues, M.M., Ballintine, E.J., Wiggert, B.N., Lee, L., Fletcher, R.T. and Chader, G.J. Choroideremia: a clinical, electron microscopic, and biochemical report. *Ophthalmology* 91:873-883, 1984.

70. Rosenberg, T., Schwartz, M., Niebuhr, E., et al. Choroideremia in interstitial deletion of the X chromosome. *Ophthalmic Paediatr.Genet.* 7:205-210, 1986.

71. Sanford, J.C., Pan, Y. and Wessling-Resnick, M. Properties of Rab5 N-terminal domain dictate prenylation of C-terminal cysteines. *Mol.Biol.Cell* 6:71-85, 1995a.

72. Sanford, J.C., Yu, J., Pan, J.Y. and Wessling-Resnick, M. GDP dissociation inhibitor serves as a cytosolic acceptor for newly synthesized and prenylated Rab5. *J.Biol.Chem.* 270:26904-26909, 1995b.

73. Sankila, E.M., de la Chapelle, A., Karna, J., Forsius, H., Frants, R. and Eriksson, A. Choroideremia: close linkage to DXYS1 and DXYS12 demonstrated by segregation analysis and historical-genealogical evidence. *Clin.Genet.* 31:315-322, 1987.

74. Schalk, I., Zeng, K., Wu, S.K., et al. Structure and mutational analysis of Rab GDP-dissociation inhibitor. *Nature* 381:42-48, 1998.

75. Schwartz, M., Yang, H.M., Niebuhr, E., Rosenberg, T. and Page, D.C. Regional localization of polymorphic DNA loci on the proximal long arm of the X chromosome using deletions associated with choroideremia. *Hum.Genet.* 78:156-160, 1988.

76. Seabra, M.C. New insights into the pathogenesis of choroideremia: a tale of two REPs [editorial; comment]. *Ophthalmic Genet.* 17:43-46, 1996.

77. Seabra, M.C., Brown, M.S. and Goldstein, J.L. Retinal degeneration in choroideremia: deficiency of rab geranylgeranyl transferase. *Science* 259:377-381, 1993a.

78. Seabra, M.C., Brown, M.S., Slaughter, C.A., Sudhof, T.C. and Goldstein, J.L. Purification of component A of Rab geranylgeranyl transferase: possible identity with the choroideremia gene product. *Cell* 70:1049-1057, 1992a.

79. Seabra, M.C., Goldstein, J.L., Sudhof, T.C. and Brown, M.S. Rab Geranylgeranyl Transferase, a multisubunit enzyme that prenylates GTP-binding proteins terminating in Cys-X-Cys or Cys-Cys. *J.Biol.Chem.* 267:14497-14503, 1992b.

80. Seabra, M.C., Ho, Y.K. and Anant, J.S. Deficient geranylgeranylation of Ram/Rab27 in choroideremia. *J.Biol.Chem.* 270:24420-24427, 1995.

81. Shen, F. and Seabra, M.C. Mechanism of digeranylgeranylation of Rab proteins. Formation of a complex between monogeranylgeranyl-Rab and Rab escort protein. *J.Biol.Chem.* 271:3692-3698, 1996.

82. Siu, V.M., Gonder, J.R., Jung, J.H., Sergovich, F.R. and Flintoff, W.F. Choroideremia associated with an X-autosomal translocation. *Hum.Genet.* 84:459-464, 1990.

83. Sogaard, M., Tani, K., Ye, R.R., et al. A rab protein is required for the assembly of SNARE complexes in the docking of transport vesicles. *Cell* 78:937-948, 1994.

84. Soldati, T., Riederer, M.A. and Pfeffer, S.R. Rab GDI: a solubilizing and recycling factor for rab9 protein. *Mol.Biol.Cell* 4:425-434, 1993.

85. Soldati, T., Shapiro, A.D., Svejstrup, A.B. and Pfeffer, S.R. Membrane targeting of the small GTPase Rab9 is accompanied by nucleotide exchange [see comments]. *Nature* 369:76-78, 1994.

86. Sorsby, A., Franceschetti, A., Joseph, R. and Davey, J.B. Choroideremia: clinical and genetic aspects. *Br.J.Ophthalmol.* 36:547-581, 1952.

87. Ullrich, O., Horiuchi, H., Bucci, C. and Zerial, M. Membrane association of Rab5 mediated by GDP-dissociation inhibitor and accompanied by GDP/GTP exchange. *Nature* 368:157-160, 1994a.

88. van Bokhoven, H., Schwartz, M., Andreasson, S., et al. Mutation spectrum in the CHM gene of Danish and Swedish choroideremia patients. *Hum.Mol.Genet.* 3:1047-1051, 1994a.

89. van Bokhoven, H., van den Hurk, J.A., Bogerd, L., et al. Cloning and characterization of the human choroideremia gene. *Hum.Mol.Genet.* 3:1041-1046, 1994b.

90. van den Hurk, J.A., Hendriks, W., van de Pol, D.J., et al. Mouse choroideremia gene mutation causes photoreceptor cell degeneration and is not transmitted through the female germline. *Hum.Mol.Genet.* 6:851-858, 1997a.

91. van den Hurk, J.A., Schwartz, M., van Bokhoven, H., et al. Molecular basis of choroideremia (CHM): mutations involving the Rab escort protein-1 (REP-1) gene. *Hum.Mutat.* 9:110-117, 1997b.

92. van den Hurk, J.A., van de Pol, T.J., Molloy, C.M., et al. Detection and characterization of point mutations in the choroideremia candidate gene by PCR-SSCP analysis and direct DNA sequencing. *Am.J.Hum.Genet.* 50:1195-1202, 1992.

93. Waldherr, M., Ragnini, A., Schweyer, R.J. and Boguski, M.S. MRS6--yeast homologue of the choroideraemia gene [letter]. *Nat.Genet.* 3:193-194, 1993.

94. Warren, W., Hovig, E., Smith-Sorensen, B., et al. Searching Candidate Genes for Mutations. In: *Current Protocols in Human Genetics*, edited by Dracopoli, N.C., Haines, J.L., Korf, B.R., et al. Massachusetts: John Wiley & Sons, Inc., 1997, p. 7.4.1-7.4.4

95. Wilson, A.L., Erdman, R.A. and Maltese, W.A. Association of Rab 1B with GDP-dissociation inhibitor (GDI) is required for recycling but no initial membrane targeting of the rab protein. *J.Biol.Chem.* 271:10932-10940, 1996.

96. Wong, P. Lateral genetics: An approach to the cloning of potential human chorio-retinal X-linked genes. 1992. University of Ottawa. (GENERIC)
Ref Type: Thesis/Dissertation

97. Wright, A.F., Nussbaum, R.L., Bhattacharya, S.S., et al. Linkage studies and deletion screening in choroideremia. *J.Med.Genet.* 27:496-498, 1990.

98. Zhang, F.L. and Casey, P.J. Protein prenylation: molecular mechanisms and functional consequences. *Annu.Rev.Biochem.* 65:241-269, 1996.

Protein	Localization	Function
Rab1A, 1B	ER, Golgi intermediate compartment	ER→Golgi transport; intra-Golgi transport
Rab2	ER, Golgi intermediate compartment	ER→Golgi transport
Rab3A	Synaptic vesicles; chromaffin granules	Regulated exocytosis in pancreatic acinar cells, adrenal chromaffin cell and mast cells
Rab3B	Tight junction region in polarized epithelial cells	not determined
Rab3C	Synaptic vesicles	not determined
Rab 3D	Zymogen granules in pancreatic acinar cells	not determined
Rab4A, Rab4B	Early endosomes	Recycling pathway from endosomes to plasma membrane
Rab5A, Rab5B, Rab5C	Plasma membrane; clathrin-coated vesicles; early endosomes	Plasma membrane→early endosome transport; homotypic fusion between early endosomes
Rab6	Middle Golgi, TGN	Intra-Golgi retrograde transport
Rab7	Late endosomes	Transport from early to late endosomes and lysosomes
Rab8	Post-Golgi exocytic vesicles; tight junction in epithelial cells	Golgi→plasma membrane transport
Rab9	Late endosomes and TGN Golgi complex	Transport from late endosomes to TGN
Rab10	TGN; constitutive secretory vesicles;	not determined
Rab11	secretory granules; recycling endosomes	Transport through recycling endosomes
Rab27	not determined	Putative transport of substrates within RPE, choriocapillaris and retina

Table 1-1. Location and function of Rab proteins in mammalian cells. (ER=endoplasmic reticulum, TGN=Trans-golgi network) Modified after Novick and Zerial, 1997.

exon	oligonucleotide (5'→3')	orientation	size (bp)	t_a (°C)
1	GACCTTCCACCCAAGAACTAC	sense	216	59
	ACAGTCTTCCTAAACTTTGTCC	antisense		
2	TGTTCTATACAGCAATGGCA	sense	190	51
	GGAAATATTAAATGCTATCGTT	antisense		
3	TTGATGAAGATCAGTGAATTG	sense	179	54
	CAAAGCAAATTAAAAGGTCAG	antisense		
4	TTGCATGTTTCACACTGCCCAC	sense	222	61
	AGTCATTAATTTAGTTTACCTGCAG	antisense		
5a	AGCCTGGTGTTTATTATTATATT	sense	246	53
	GTCACTTCAGCACCATTTAC	antisense		
5b	GATCCAGAGAATGCGCTAG	sense	246	53
	GCAAAGATGGGTAAAATTAGT	antisense		
6	CCAATTTTTCTACTATTTCAAC	sense	214	51
	AACTTAAGCTGATGCCCAGT	antisense		
7	AGTTATATCATTAGGAAGCAG	sense	206	51
	TTGGAGAGCACTACTTAATG	antisense		
8	AGTTTAGTTCTGATTTTAAGTG	sense	309	53
	CACTTTTAGAAGGGACAAGAA	antisense		
9	TTTTCAACCCAATTACCCTA	sense	156	51
	TATATATGAAGGTTACTTATATC	antisense		
10	ATGAACTTTTATGGTATGCTTATCTT	sense	185	61
	GTCAATAAAATTACCTTCGCTTGC	antisense		
11	CGAACTTATCCATGGAATC	sense	207	55
	ccgGTGTAGTGATTAGTTCACCA	antisense		
12	cGATCTAACAGCTGTGTCTGAT	sense	174	55
	ccggAAAATACAAATAACCACTCT	antisense		
13	cGCTCAGCTCTCTATTATCCAT	sense	258	55
	ccgGAAGATTATGATGGTTACAT	antisense		
14	cgTAGGCTACACAGTGTAGTAA	sense	322	55
	ccgGACTTCTCTCCTCCCAGAGG	antisense		
15	AGTTAATGCCAGAAAATGCAC	sense	289	55
	ccGGGTATCCAGTTTGGTGTATA	antisense		

Table 2-1. Oligonucleotide primers used for PCR amplification of CHM exons (van Bokhoven et al., 1994).

Family	Position		Mutation	Effect
1	Exon 7	907	C→T	R293stop
2	Exon 5	555-556	del AG	frameshift
3	Exon 6	787	C→T	R253stop
4	Exon 1	45	del C	frameshift
5	Exons 5→8		intragenic deletion	truncated product

Table 4-1. Summary table showing mutations in the REP-1 gene discovered in this study.

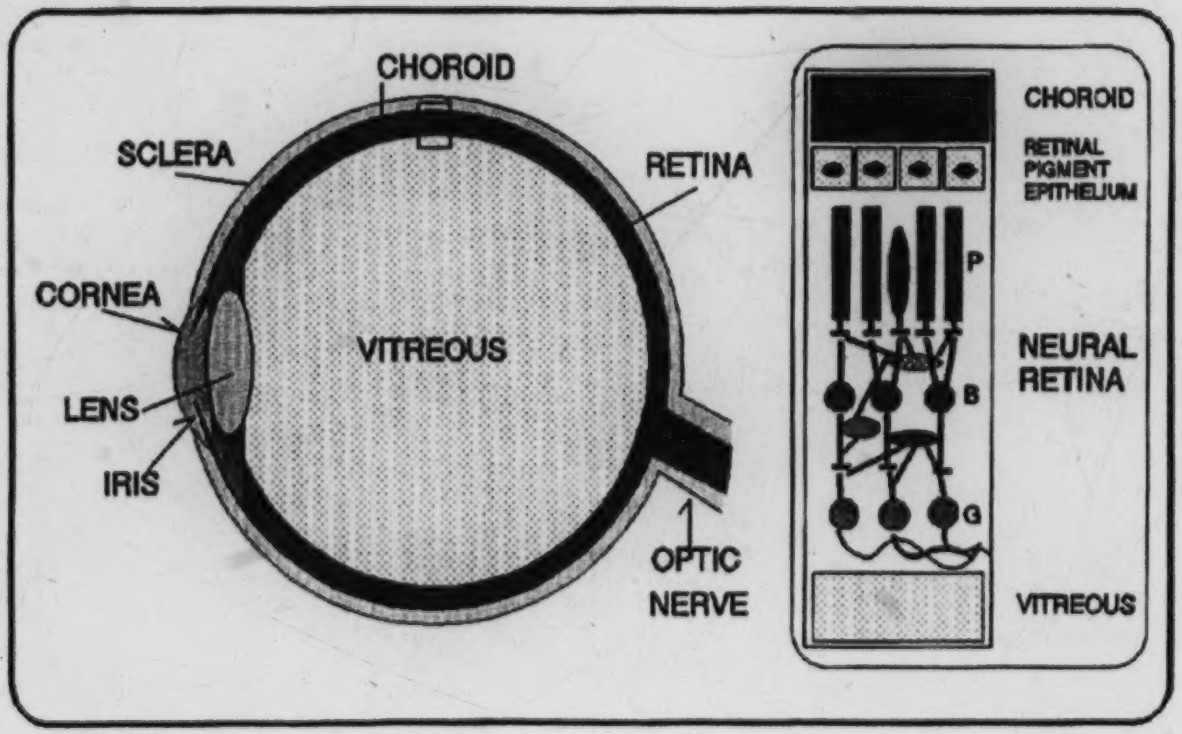

Figure 1-1. Cross-sectional diagram of the eye. Three distinct layers are shown – the photoreceptor layer, retinal pigment epithelium (RPE) and the choroid. Figure adapted from Wong, 1992.

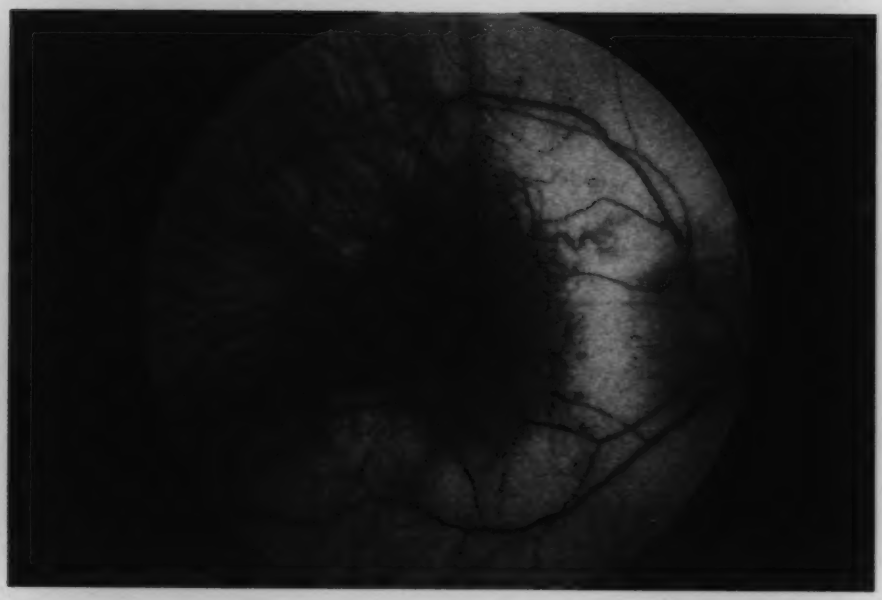

Figure 1-2. Fundus photograph taken from an affected male.

Figure 1-3. Fundus photograph taken from a carrier female.

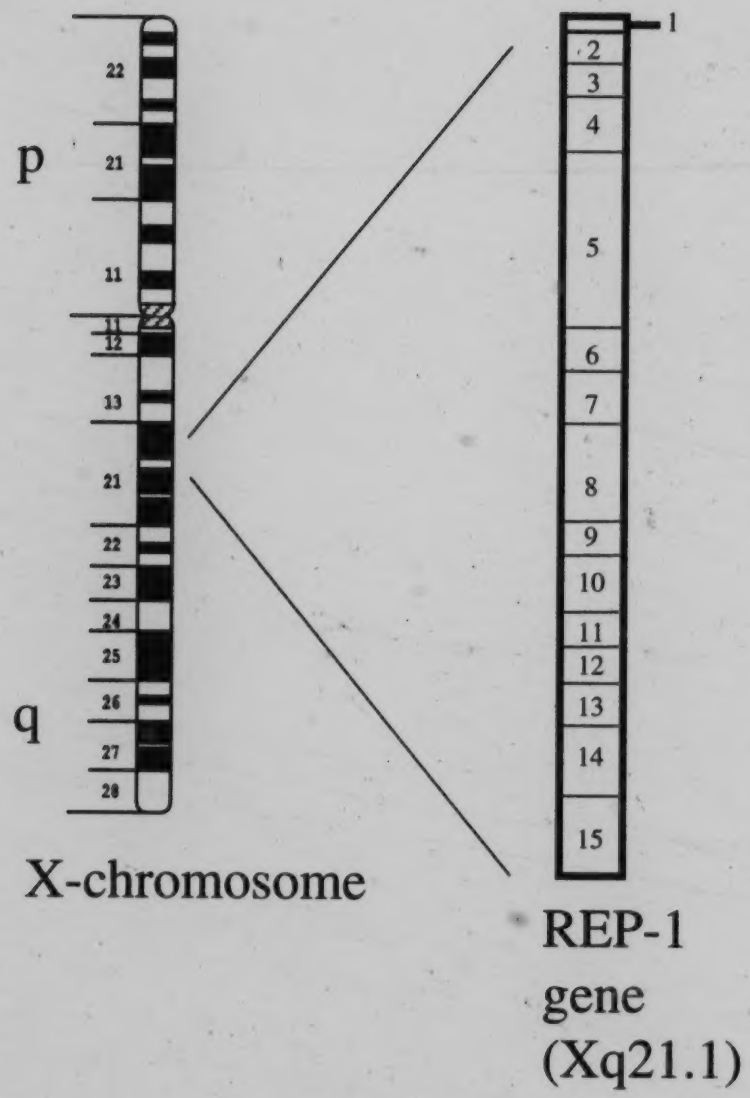

Figure 1-4. Position of the CHM gene on the X-chromosome and structure of the open reading frame.

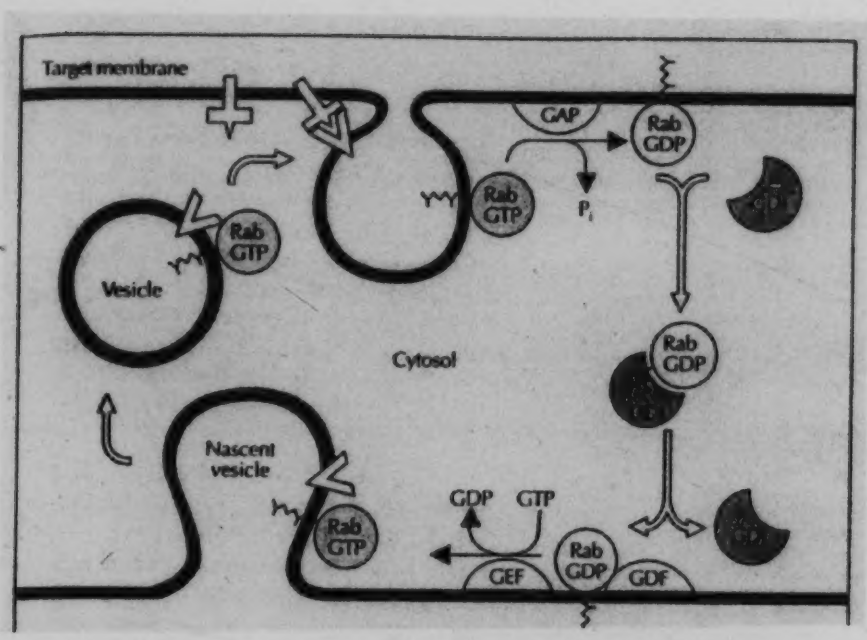

Figure 1-5. Rab protein involvement in membrane trafficking. Prenylated Rabs are initially located in the cytosol complexed with Rab guanine-nucleotide dissociation inhibitor (GDI). Rab GDI escorts the Rab protein to a specific organelle membrane. A GDI-displacement factor (GDF) may help release Rab GDI from the Rab protein. A guanine-nucleotide exchange factor (GEF) replaces bound GDP with GTP, activating the Rab protein. Rab proteins, with GTP bound, now catalyze the interaction between appropriate v-SNAREs and t-SNAREs, and allow proper association between vesicle and target membrane. After the fusion event has occurred, and transfer of vesicular contents into target organelle, a GTPase activating protein (GAP) converts the Rab protein back into its GDP-bound form, deactivating the protein. A free Rab-GDI protein then retrieves the Rab protein and delivers it to its original cellular compartment so that another round of vesicular transport can occur. Adapted after Pfeffer, 1994.

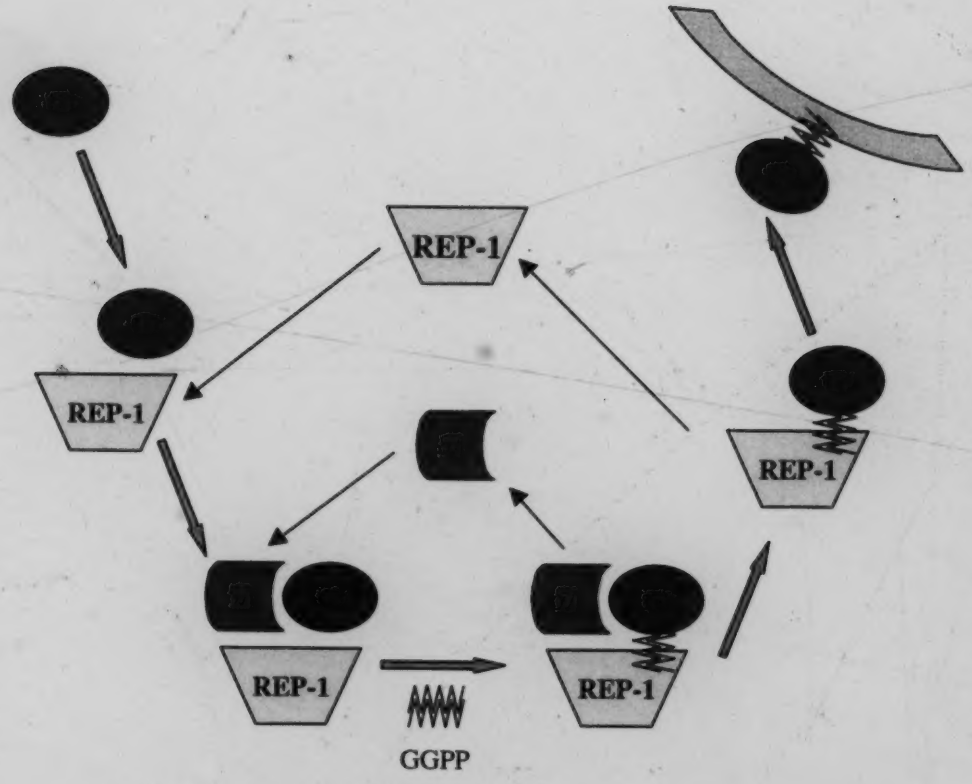

Figure 1-6. The role of the REP-1 protein in the geranylgeranylation of Rab proteins. (Rab=Rab protein, REP-1=Rab Escort Protein – 1, α/β=2 subunits of Rab geranylgeranylgransferase, GGPP=geranylgeranylpyrophosphate)

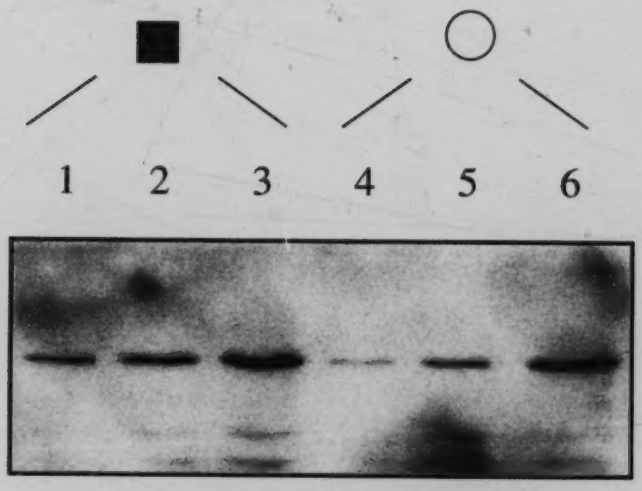

Figure 3-1. Western analysis of serial dilutions of lymphocyte protein taken from a normal male (lanes 1-3) and a normal female (lanes 4-6). The amounts of protein loaded into each lane are as follows: lane 1 – 14 μg; lane 2 – 28 μg; lane 3 – 42 μg; lane 4 – 7 μg; lane 5 – 14 μg; lane 6- 21 μg.

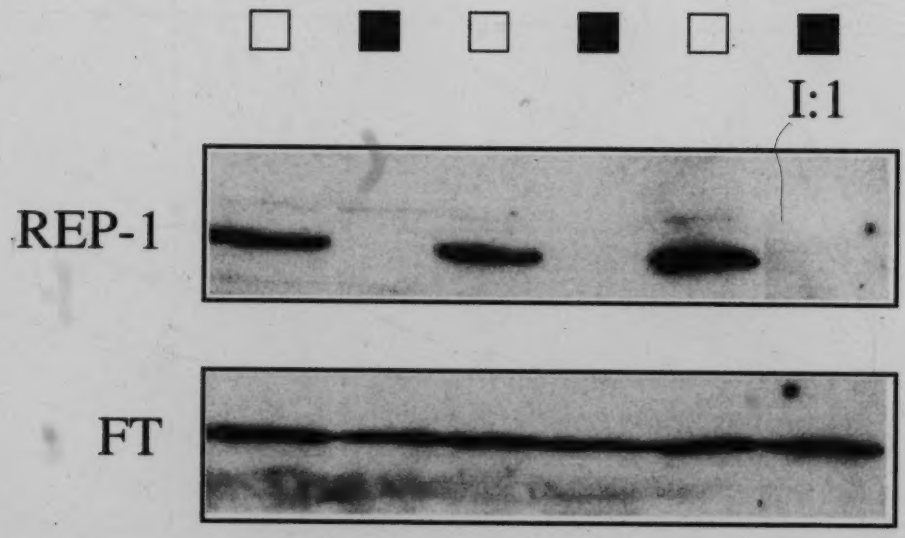

Figure 3-2. Western analysis performed on lymphocyte protein taken from affected individual I:1 from family 1, showing the absence of REP-1 protein. Protein from unrelated normal and affected individuals is also seen on this western blot, confirming the reliability of the test. The membrane was probed with monoclonal antibodies against REP-1 (upper pannel) and the α-subunit of farnesyl transferase (lower panel) which served as a loading control. Symbols represent the gender and status of the individual. (□ - normal male; ■ - affected male; ◯ - normal female; ⦿ - carrier female)

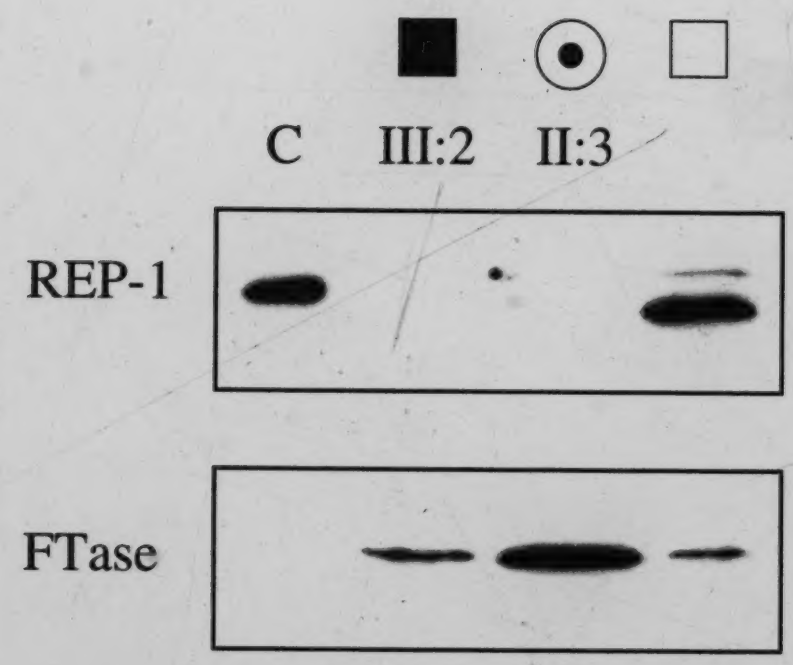

Figure 3-3. Western analysis performed on lysates taken from lymphoblasts clearly demonstrating the absence of REP-1 protein in the affected individual III:2 from family 2. His mother II:3 displayed no REP-1 product. Recombinant rat REP-1 protein served as a loading control. (C=control lane)

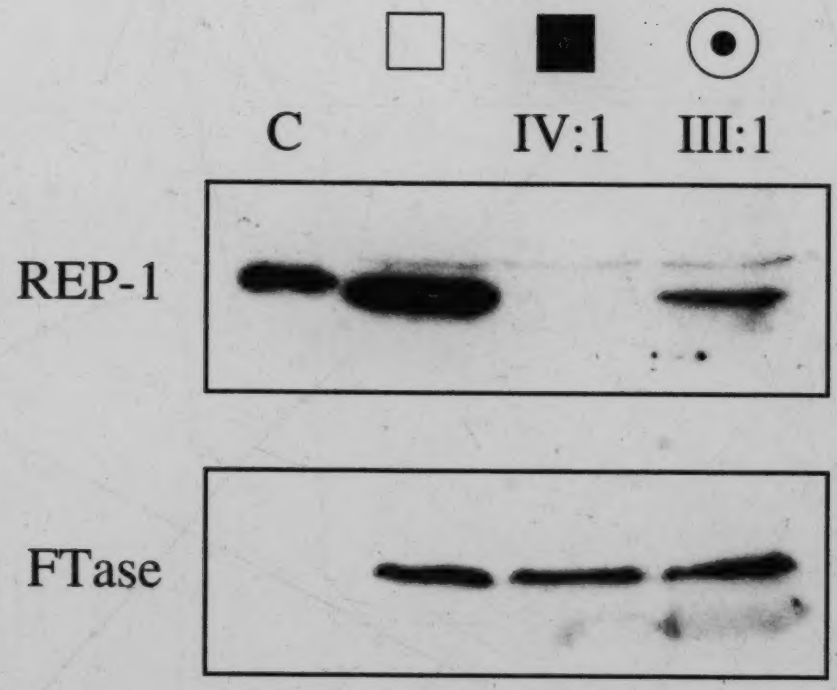

Figure 3-4. Western analysis performed on lymphoblast protein shows that affected individual IV:1 from family 3 lacks detectable REP-1 protein. His mother III:1, a female carrier, shows slightly lower REP-1 expression when compared to that of a normal individual.

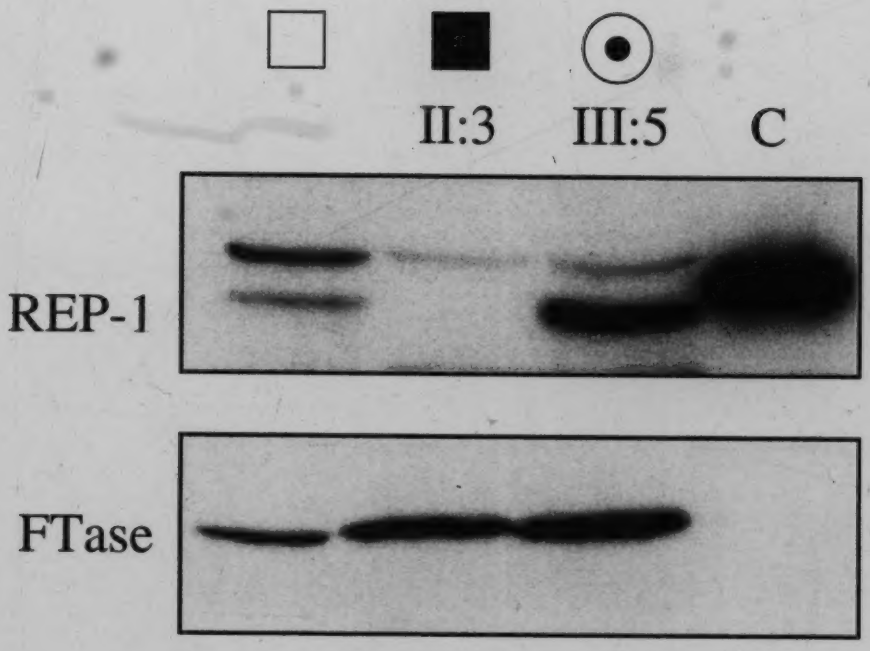

Figure 3-5. Western analysis of protein extracted from lymphocytes, showing absence of REP-1 protein in affected individual II:3 from family 4. Both his daughter, female carrier III:5 and the normal control individual demonstrate the normal amount of REP-1.

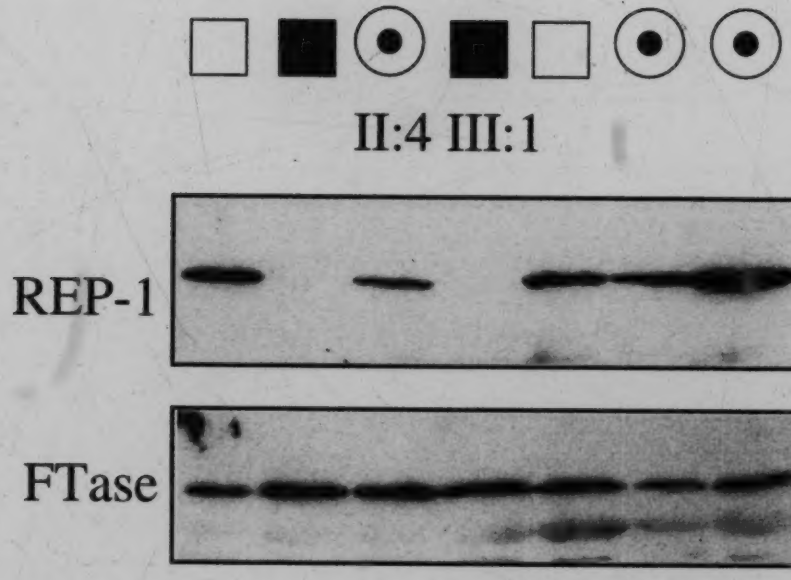

Figure 3-6. Western analysis on lymphocyte protein showed that REP-1 protein is absent from affected individual III:1 from family 5. Unrelated normal, affected and carrier individuals are also shown on this western blot.

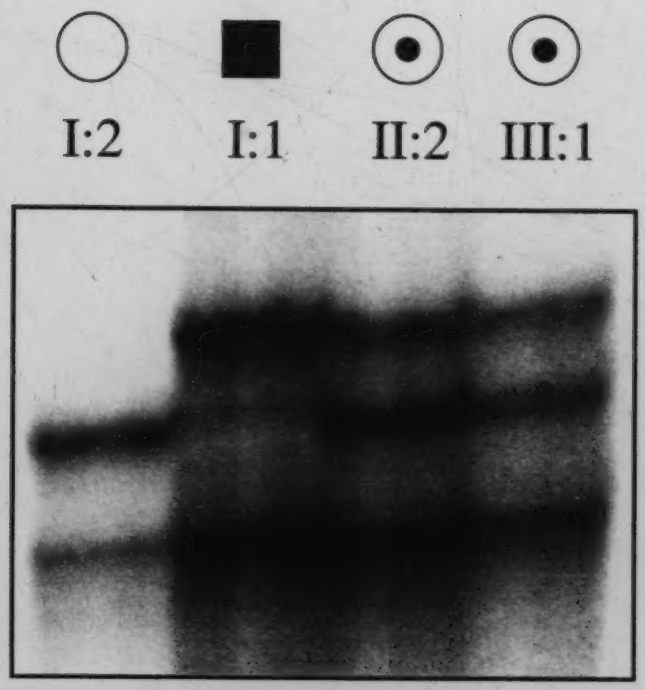

Figure 3-7. SSCP analysis of exon 7 showing a band shift in affected individual I:1 from family 1, when compared to that of his normal wife I:2. Also shown is the heterozygous banding pattern present in the two female carriers, his daughter II:2 and granddaughter III:1.

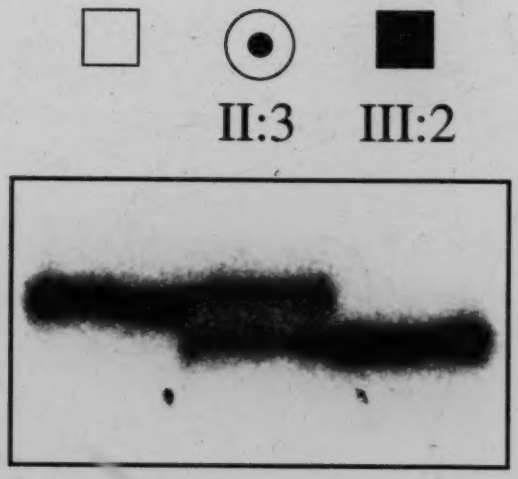

Figure 3-8. SSCP analysis demonstrating a band shift in exon 5 in affected individual III:2 from family 2 as compared to the normal banding pattern. A heterozygous banding pattern is shown in female carrier II:3.

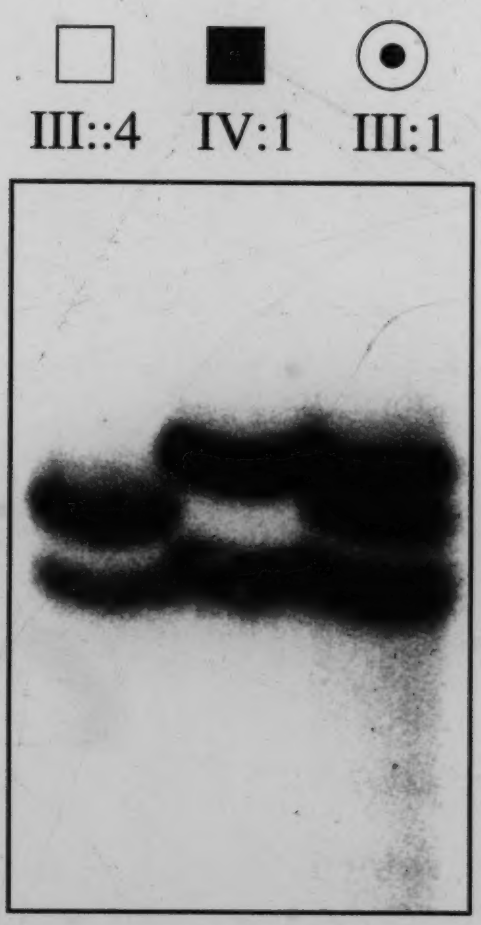

Figure 3-9. SSCP analysis of exon 6 showing a band shift in affected individual IV:1 from family 3, and the heterozygous banding pattern in the female carrier III:1.

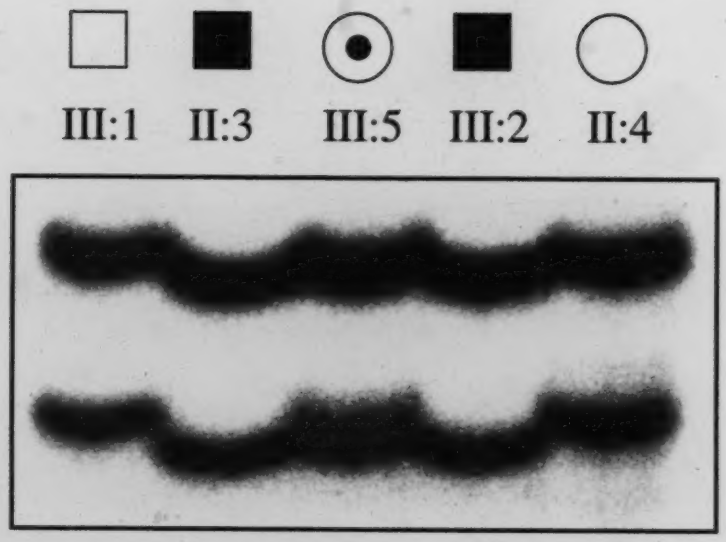

Figure 3-10. In affected individuals II:3 and III:2, both from family 4, SSCP analysis detects a band shift in exon 1. Female carrier III:5 shows the heterozygous banding pattern, while normal individuals III:1 and II:4 both show wild-type banding patterns.

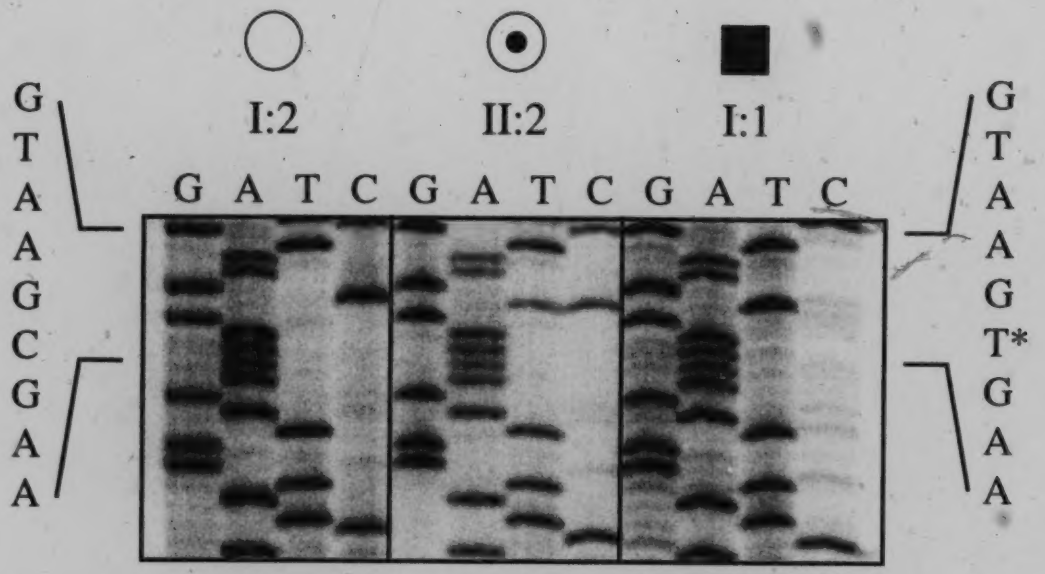

Figure 3-11. Partial sequence analysis of exon 7, showing a C to T transition mutation at position 907 in individual I:1 from family 1. His wife I:2 shows normal sequence, while his carrier daughter displays heterozygosity for the mutation.

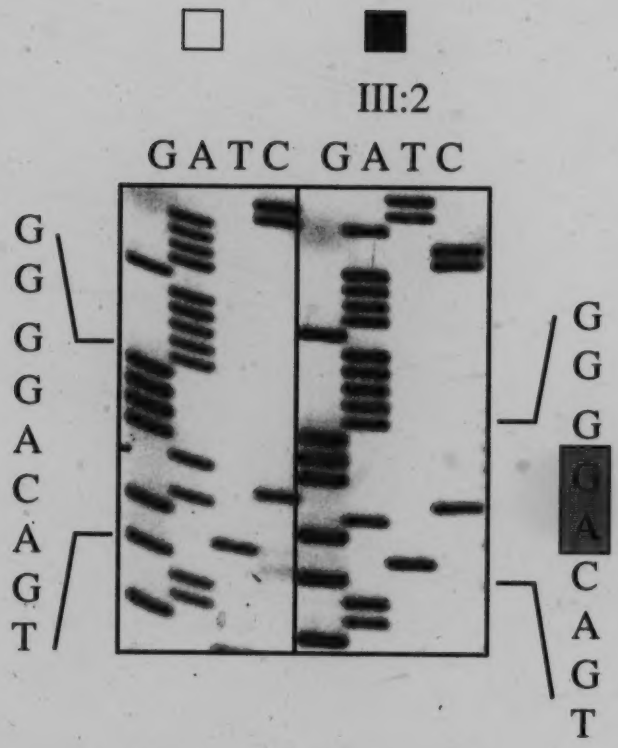

Figure 3-12. Partial sequence analysis of exon 5 showing a 2 base AG deletion at cDNA position 555/556, in affected individual III:2 from family 2.

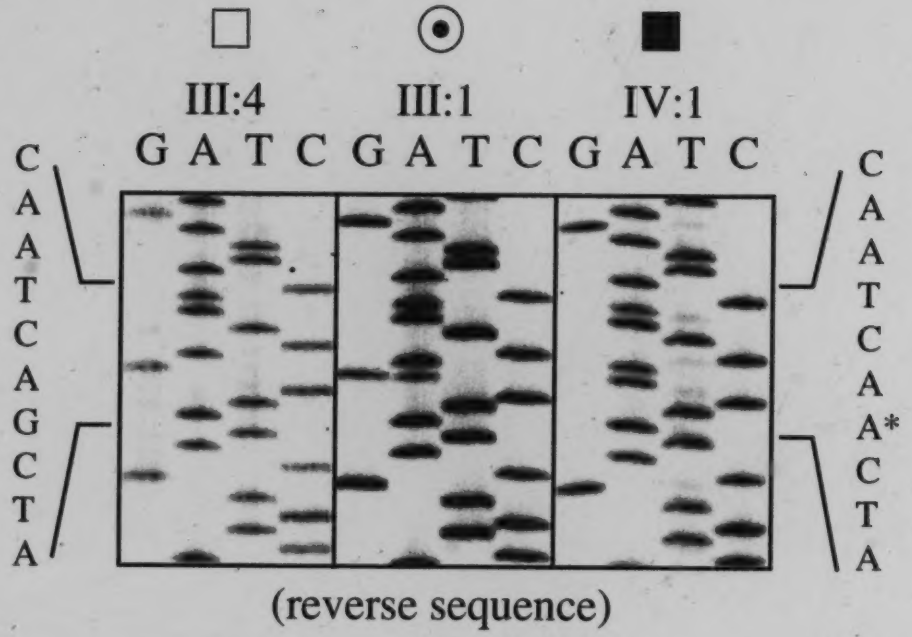

Figure 3-13. Partial sequence data from exon 6 taken from the reverse strand. Affected individual IV:1 from family 3 shows a base change corresponding to a C to T transition mutation at position 787, while the female carrier III:1 is heterozygous for the mutation.

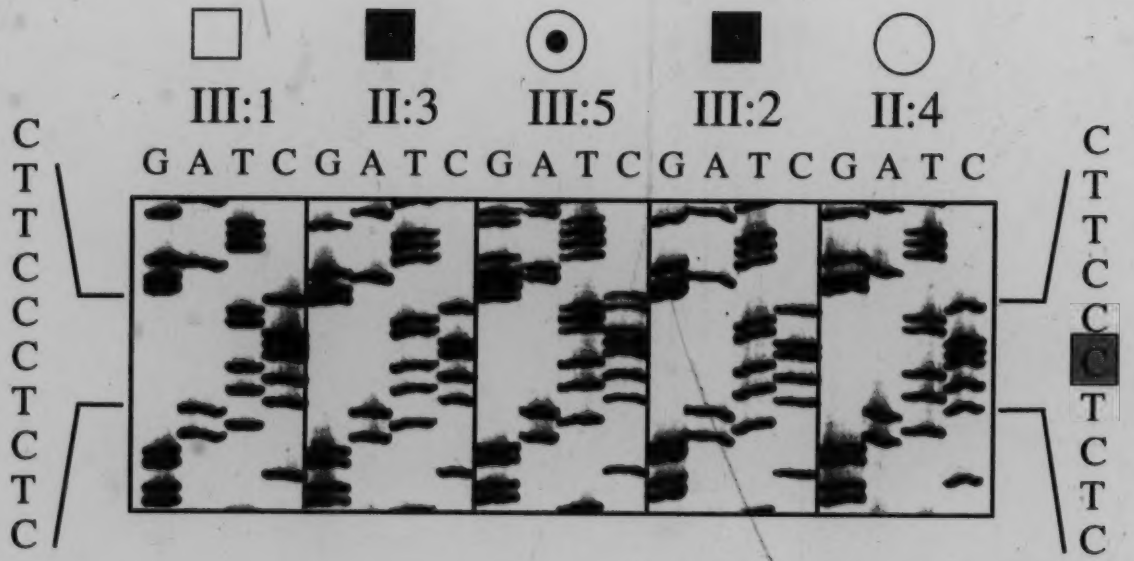

Figure 3-14. Partial sequence analysis of exon 1 displays a C deletion at position 45 in affected individuals II:3 and III:2 from family 4. The sequence misalignment in the female carrier III:5 occurring immediately after this base deletion corresponds to heterozygosity for this mutation. Both II:4 and III:1 show normal sequence.

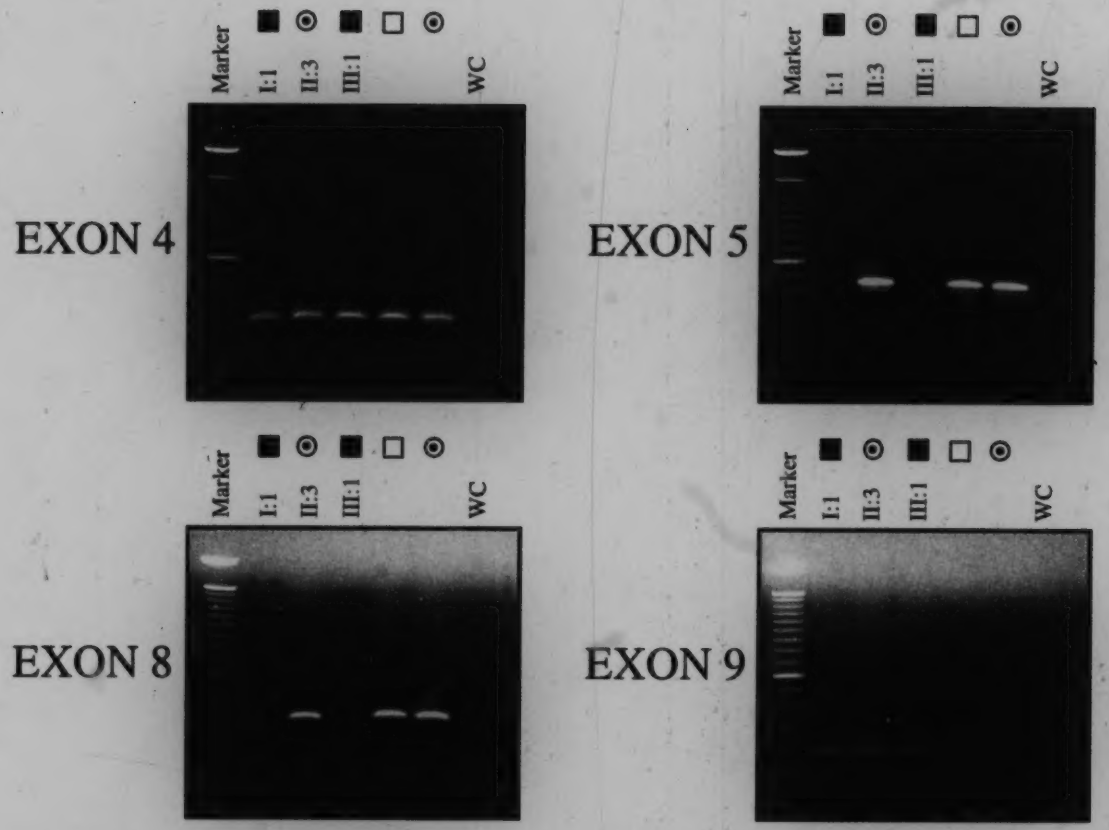

Figure 3-15. PCR amplification of specific exons 4, 5, 8 and 9 done on individuals from family 5. The results clearly demonstrate the absence of exons 5 and 8 in affected individuals I:1 and III:1 from this family, suggesting an intragenic deletion involving exons 5 to 8. A 100 bp ladder was utilized in order to confirm appropriate exon sizes.

a)

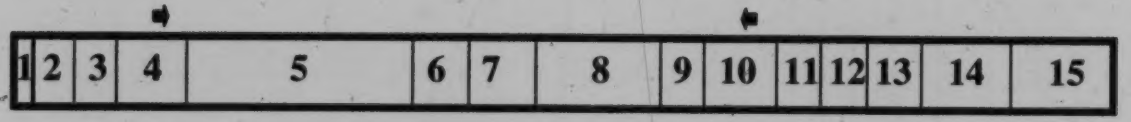

b)

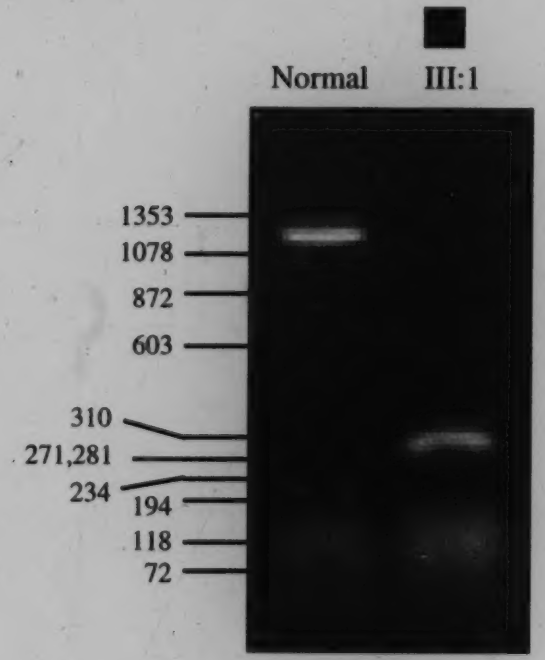

Figure 3-16a. Location of the exonic PCR primers used for RT-PCR.
Figure 3-16b. RT-PCR results using exonic primers flanking exons 5 and 8. The presence of a smaller size band in the affected male III:1 from family 5, confirms a deletion. The appropriate marker sizes are shown on the side.

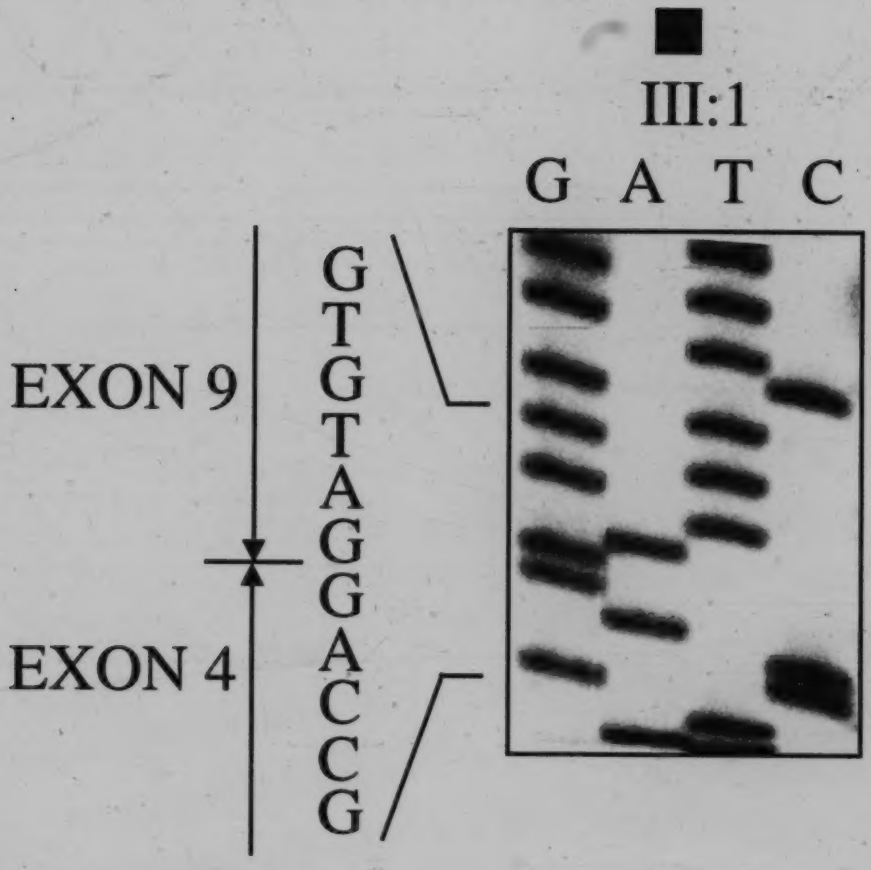

Figure 3-17. Direct sequence of the smaller fragment seen in affected individual III:1 from family 5, confirming the absence of exons 5 to 8 in the mRNA product.

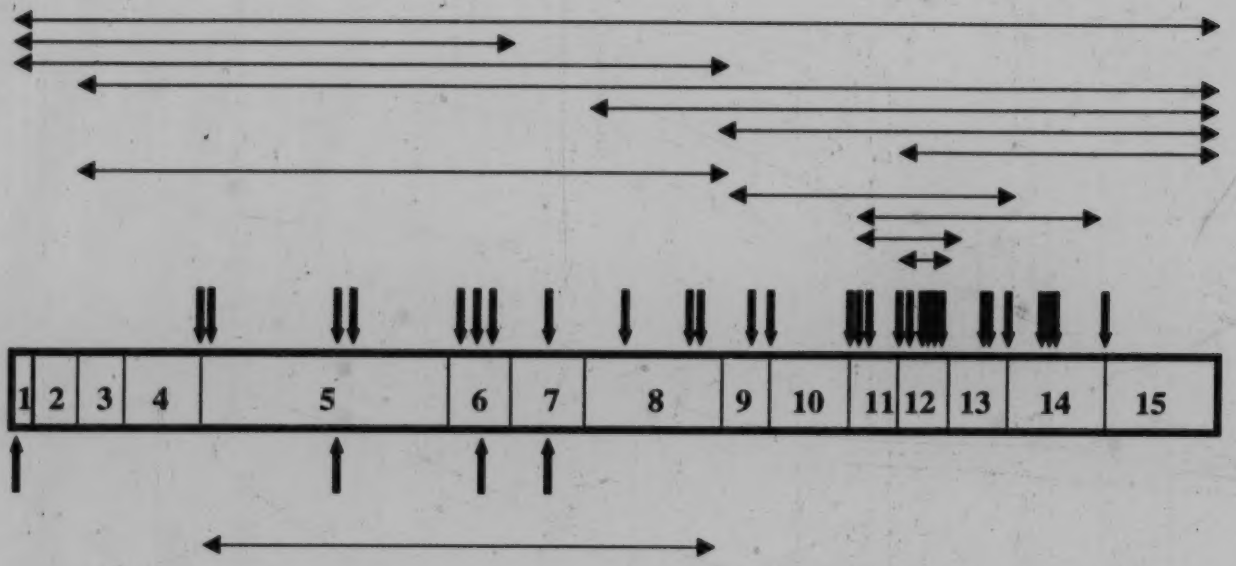

Figure 4-1. Locations of previously published mutations (above the coding region) in comparison to the mutations described in this work (below the coding region)